1992-09

Flexural wave propagation in anisotropic laminates and inversion algorithms to recover elastic constants

Elliott, Brian B.

Monterey, California. Naval Postgraduate School

REPORT DOCUMENTATION PAGE

1a. REPORT SECURITY CLASSIFICATION UNCLASSIFIED	1b. RESTRICTIVE MARKINGS
2a. SECURITY CLASSIFICATION AUTHORITY	3. DISTRIBUTION/AVAILABILITY OF REPORT Approved for public release; distribution is unlimited.
2b. DECLASSIFICATION/DOWNGRADING SCHEDULE	
4. PERFORMING ORGANIZATION REPORT NUMBER(S)	5. MONITORING ORGANIZATION REPORT NUMBER(S)
6a. NAME OF PERFORMING ORGANIZATION Naval Postgraduate School 6b. OFFICE SYMBOL (*If applicable*) 55	7a. NAME OF MONITORING ORGANIZATION Naval Postgraduate School
6c. ADDRESS (*City, State, and ZIP Code*) Monterey, CA 93943-5000	7b. ADDRESS (*City, State, and ZIP Code*) Monterey, CA 93943-5000
8a. NAME OF FUNDING/SPONSORING ORGANIZATION 8b. OFFICE SYMBOL (*If applicable*)	9. PROCUREMENT INSTRUMENT IDENTIFICATION NUMBER
8c. ADDRESS (*City, State, and ZIP Code*)	10. SOURCE OF FUNDING NUMBERS Program Element No. / Project No. / Task No / Work Unit Accession Number

11. TITLE (*Include Security Classification*)
FLEXURAL WAVE PROPAGATION IN ANISOTROPIC LAMINATES AND INVERSION ALGORITHMS TO RECOVER ELASTIC CONSTANTS USING PHASE VELOCITY MEASUREMENTS

12. PERSONAL AUTHOR(S) Brian B. Elliott

13a. TYPE OF REPORT	13b. TIME COVERED	14. DATE OF REPORT (*year, month, day*)	15. PAGE COUNT
Master's Thesis	From To	September 1992	67

16. SUPPLEMENTARY NOTATION
The views expressed in this thesis are those of the author and do not reflect the official policy or position of the Department of Defense or the U.S. Government.

17. COSATI CODES			18. SUBJECT TERMS (*continue on reverse if necessary and identify by block number*)
FIELD	GROUP	SUBGROUP	anisotropy;composites;flexural waves;elastic constants

19. ABSTRACT (*continue on reverse if necessary and identify by block number*)

Knowledge of the elastic properties of composite materials can be an invaluable tool for both the quality asurance of manufacturing techniques and design verification. Recent advances in ultrasonic velocity measurements have demonstrated the ability to recover elastic properties in anisotropic lamiantes. A simplified experimental setup was investigated to recover the elastic properties based upon the flexural wave propagation in anisotopic laminates. The initial objective of this thesis was to verify flexural wave propagation in composite laminates through the comparision of experimental and theoretical phase velocities. In the second part of this thesis, the experimental phase velocites were used to calculate the elastic properties of the material by inverting the governing equations. The initial method used to recover elastic constants was successful in the recovery of a partial set of the bending and extensional stiffnesses. The inability to recover all bending stiffnesses dictated the investigation of asecond method. This method used an iterative method based uipon a nonlinear Newton's method to recover the bending stiffnesses. This method did not converge due to the ill conditioning of the solution matrix. Although this method did not converge, it is believed that more robust methods suggested herein would converge to the proper solution.

20. DISTRIBUTION/AVAILABILITY OF ABSTRACT	21. ABSTRACT SECURITY CLASSIFICATION	
☒ UNCLASSIFIED/UNLIMITED ☐ SAME AS REPORT ☐ DTIC USERS	Unclassified	
22a. NAME OF RESPONSIBLE INDIVIDUAL Michael R. Gorman	22b. TELEPHONE (*Include Area code*) 408-646-2889	22c. OFFICE SYMBOL 31

DD FORM 1473, 84 MAR — 83 APR edition may be used until exhausted; All other editions are obsolete

Approved for public release; distribution is unlimited.

Flexural Wave Propagation in Anisotropic Laminates and Inversion Algorithms to Recover Elastic Constants

by

Brian B. Elliott
Lieutenant, United States Navy
B.M.E., Villanova University, 1983

Submitted in partial fulfillment
of the requirements for the degree of

MASTER OF SCIENCE IN AERONAUTICAL ENGINEERING

from the

ABSTRACT

Knowledge of the elastic properties of composite materials can be an invaluable tool for both the quality assurance of manufacturing techniques and design verification. Recent advancements in ultrasonic velocity measurements have demonstrated the ability to recover elastic properties in anisotropic laminates. A simplified experimental setup was investigated to recover the elastic properties based upon the flexural wave propagation in anisotropic laminates. The initial objective of this thesis was to verify flexural wave propagation in composite laminates through the comparison of experimental and theoretical phase velocities. In the second part of this thesis, the experimental phase velocities were used to calculate the elastic properties of the material by inverting the governing equations. The initial method used to recover elastic constants was successful in the recovery of a partial set of the bending and extensional stiffnesses. The inability to recover all bending stiffnesses dictated the investigation of a second method. This method used an iterative method based upon a nonlinear Newton's method to recover the bending stiffnesses. This method did not converge due to ill conditioning of the solution matrix. Although this method did not converge, it is believed that other more robust methods suggested herein would converge to the proper solution.

TABLE OF CONTENTS

I. INTRODUCTION

Composite materials have been used quite extensively in the past for high performance structural components and promise to be major structural materials of the future [Refs. 1-4]. The inherent advantage of composite materials is their high strength to weight ratio. Composite structures present unique problems in that these materials are produced by complex manufacturing processes. These processes include a large number of manufacturing variables which increase the number of opportunities for introduction of defects. Variables such as state of cure of the resin, fiber to matrix bond, and fiber to resin ratio have an effect on the elastic properties of a laminate. It is thus imperative that controlled procedures be established for quality assurance throughout the manufacturing process. A knowledge of the elastic properties of composite materials would be invaluable for both design verification and quality assurance. There is a need for a simple and quick in situ test which can yield quantitative parameters descriptive of the mechanical state of the material.

Several non-destructive testing (NDT) techniques with their own inherent strengths and weaknesses are currently available to assess the mechanical states of composites and are discussed below.

Radiographical techniques have long been available to detect large voids, porosity content, foreign debris and other imperfections in composite laminates. The presence of these imperfections has a most definite impact upon the material properties. There seems to be disagreement on the ability of radiography to determine fiber volume while the value of this technique reduces with increased laminate thickness. [Ref. 4]

Ultrasonic methods are one of the most widely employed techniques for the non-destructive testing of composite laminates [Ref. 5-10]. Ultrasonic NDT techniques include velocity measurement, ultrasonic spectroscopy and attenuation measurement.

There is a definite relationship between void content and mechanical strength. Ultrasonic spectroscopy has proven itself to be a viable technique to detect and locate voids, delaminations and other defects. Also, the dependence of ultrasonic attenuation upon void content has been clearly demonstrated. While these NDT techniques are effective tools for testing of production quality control, they can not quantify the actual material mechanical properties. [Ref. 4]

Several works on ultrasonic velocity measurement to recover the material properties have been published recently. Dayal and Kinra [Ref. 5] verified the Lamb dispersion for an anisotropic laminate immersed in a water bath by measuring the phase velocities and attenuation of ultrasonic waves in thin plates. Every and Sachse [Ref. 6] have shown through numerical simulation it is possible to recover a partial set of elastic constants of a mildly anisotropic material using the quasi-longitudinal mode. However, the quasi-longitudinal mode is typically difficult to excite in thin plates. Wu and Ho [Ref. 7] measured the energy (group) velocity of the quasi-longitudinal and quasi-shear mode through the thickness of a 36 ply unidirectional laminate using an ultrasonic technique. The energy velocity measurements were used to calculate the phase velocities through a numerical method. From the phase velocities the elastic constants could be calculated. Wu and Chiu [Ref. 8] found good agreement between theoretical and experimental results when exciting the shear mode in a unidirectional laminate. When attempting to determine the elastic constants from

velocity measurements of the shear mode, they reported that even a small perturbation in the shear wave velocity will induce large differences in the calculated elastic constants. Castagnede *et. al.* [Ref. 9] utilized the nondispersive bulk modes to determine the elastic constants of a glass/ epoxy unidirectional composite. Every and Sachse [Ref. 10] used the group velocities of the bulk longitudinal mode to recover the elastic constants of an anisotropic solid. Every and Sachse utilized the point-source--point-receiver (PS-PR) technique to measure the group velocities. The group velocities were used to determine the elastic constants of an anisotropic solid. The PS-PR technique requires access to both sides of the specimen which is not always possible when measuring in situ.

While these methods have shown success in recovering material properties of composite laminates, there are limitations upon their usefulness to the composite community. Castagnede et. al. and Every and Sachse have proven successful in recovering elastic properties while using the bulk modes excited by the PS-PR technique. However, excitation of the bulk mode is difficult in thin plates. Wu and Ho and Wu and Chiu successfully utilized immersional ultrasonic measurements to recover the elastic constants. One drawback of this method is that the test specimen must be immersed in water.

This thesis investigates the possibility of using phase velocity measurements based on plate wave modes in thin composite laminates. The method utilizes a single pulser and receiver combination on the same side of the plate. The experimental setup does not require immersion of the specimen nor does it require access to both sides of laminate. The experimental setup is discussed in further detail in Chapter III.

Gorman [Ref. 11] has shown for this type of transmitter/receiver setup, when the wavelength is much larger than the plate thickness, only two modes of wave propagation are present with a significant amount of energy, the lowest order extensional and the flexural modes. Initially, this thesis is concerned with the verification of the dispersion curves predicted by higher order plate theory of [Ref. 12]. Experimentally measured phase velocities are compared with theoretical phase velocities calculated using the manufacturer's supplied material properties. Next, the possibility of recovering the material properties is explored through the utilization of both the classical plate theory and higher order plate theory. It is shown that by inverting the governing equations for the flexural mode, the experimentally measured phase velocities can be used to recover a partial set of the material properties of several experimental laminates.

II. WAVE THEORY FOR THIN PLATES

In the experimental section to follow, the experimentally measured phase velocities are compared to theoretical predictions. Therefore, the theory of wave propagation in thin plates must be understood. In this section, the classical plate theory and the higher order plate theory of wave propagation are presented.

A. CLASSICAL PLATE THEORY

To understand the propagation of flexural waves in thin plates, we begin by considering a plate of thickness h and of infinite extent in the x-y plane as depicted in Figure 2.1.

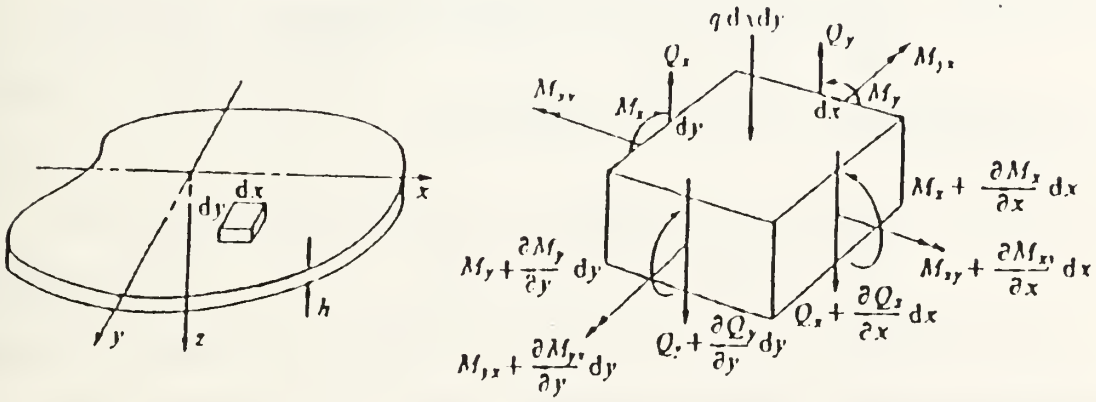

Figure 2.1 Plate Element (after Graff [Ref. 13]).

A differential element h dxdy will be subject to the various shear forces, bending and twisting moments as shown due to the applied stresses. Summing forces in the z - direction gives

$$\frac{\partial Q_x}{\partial x} + \frac{\partial Q_y}{\partial y} + q = \rho h \frac{\partial^2 w}{\partial t^2} \ . \qquad (2.1)$$

W(x,y,t,) is the displacement of the mid-plane of the plate in the z-direction. Similarly, summing moments gives

$$\frac{\partial M_y}{\partial y} - \frac{\partial M_{xy}}{\partial x} - Q_y = 0. \qquad (2.2)$$

$$\frac{\partial M_x}{\partial x} + \frac{\partial M_{xy}}{\partial y} - Q_x = 0 \qquad (2.3)$$

Solving (2.2) and (2.3) for the shear forces Q_x and Q_y and substituting into (2.1) results in a single governing equation in terms of the various moments,

$$\frac{\partial^2 M_x}{\partial x^2} + \frac{\partial M_{yx}}{\partial x \partial y} - \frac{\partial^2 M_{xy}}{\partial y \partial x} + \frac{\partial^2 M_y}{\partial y^2} + q = \rho h \frac{\partial^2 w}{\partial t^2} \ . \qquad (2.4)$$

Recognizing $M_{xy} = -M_{yx}$, (2.4) simplifies to

$$\frac{\partial M_x}{\partial x^2} + 2\frac{\partial M_{xy}}{\partial x \partial y} + \frac{\partial M_y}{\partial y^2} + q = \rho h \frac{\partial^2 w}{\partial t^2}. \qquad (2.5)$$

For a laminate arranged symmetrically about its mid plane, the bending moments are related to the curvatures by

$$\begin{bmatrix} M_x \\ M_y \\ M_{xy} \end{bmatrix} = \begin{bmatrix} D_{11} & D_{12} & D_{16} \\ D_{12} & D_{22} & D_{26} \\ D_{16} & D_{26} & D_{66} \end{bmatrix} \begin{bmatrix} K_x \\ K_y \\ K_{xy} \end{bmatrix}. \qquad (2.6)$$

The D_{ij} are the bending stiffnesses and $K_x K_y$ and K_{xy} are the middle plane curvatures which are defined as

$$\begin{bmatrix} \kappa_x \\ \kappa_y \\ \kappa_{xy} \end{bmatrix} = -\begin{bmatrix} \frac{\partial^2 w}{\partial x^2} \\ \frac{\partial^2 w}{\partial y^2} \\ \frac{\partial^2 w}{\partial x \partial y} \end{bmatrix}. \qquad (2.7)$$

The displacement of the flexural wave is given by

$$w = Ae^{i(k(l_1 x + l_2 y) - \omega t)} \qquad (2.8)$$

The value k is the wave number, l_1 and l_2, are the direction cosines in the x and y directions, respectively, ω is the circular frequency and A is the amplitude of the wave.

Substituting (2.6) through (2.8) into (2.5) and setting the body forces to zero gives

$$k^4(l_1^4 D_{11} + 4l_1^3 l_2 D_{16} + 2l_1^2 l^2 (D_{12} + 2D_{66}) + 4l_1 l_2^3 D_{26} + l_2^4 D_{22}) = \rho h \omega^2. \quad (2.9)$$

For flexural waves propagating in the x direction (i.e. l_1 =1 and l_2=0), equation (2.9) reduces to

$$k^4 D_{11} = \rho h \omega^2. \qquad (2.10)$$

Similarly, for flexural waves propagating in the y direction equation (2.9) reduces to

$$k^4 D_{22} = \rho h \omega^2. \qquad (2.11)$$

From elementary wave theory, the phase velocity, V_p, in terms of circular frequency and wave number can be written as

$$V_p = \frac{\omega}{k}. \qquad (2.12)$$

Substituting (2.12) into (2.10) and solving for the phase velocity of waves propagating in the x-direction gives

$$V_p = \left(\frac{D_{11}\omega^2}{\rho h}\right)^{\frac{1}{4}} = \left(\frac{4\pi^2 D_{11} f^2}{\rho h}\right)^{\frac{1}{4}} . \qquad (2.13)$$

Likewise, substituting (2.12) into (2.11) and solving for the phase velocity of waves propagating in the y-direction yields

$$V_p = \left(\frac{D_{22}\omega^2}{\rho h}\right)^{\frac{1}{4}} = \left(\frac{4\pi^2 D_{22} f^2}{\rho h}\right)^{\frac{1}{4}} \qquad (2.14)$$

It can be observed that the phase velocity is a function of the frequency, i.e., the phase velocity is dispersive. For low frequency conditions classical plate theory predicts the correct response. However, for short wavelength, high frequency conditions unbounded phase velocities are predicted. This physically unreasonable condition is the result of neglecting rotary inertia and shear effects in the theory.

B. HIGHER ORDER PLATE THEORY.

Classical plate theory is based on the Kirchoff hypothesis whereby the transverse shear deformation effects are neglected. However, the shear deformation effects are significant for a composite laminate owing to the fact that a composite laminate has a low transverse shear modulus. Consequently, the effects of transverse shear must be included to accurately predict the physical condition. The dispersion theory presented by Tang, Stiffler and Henneke [Ref. 12] for composite plates is an extension of the work of Mindlin [Ref. 14] performed on isotropic plates, which accounts for both transverse shear and rotary inertia corrections.

We begin our discussion of higher order plate theory by considering a composite laminate plate of thickness h with the coordinate system as presented in Fig. 2.1. The following displacement fields are assumed:

$$u = u_o(x,y,t) + z\psi_x(x,y,t) \qquad (2.15)$$

$$v = v_o(x,y,t) + z\psi_y(x,y,t) \qquad (2.16)$$

$$w=w(x,y,t). \qquad (2.17)$$

The displacement coordinates u, v, and w are in the x, y, and z directions, u_o and v_o are the mid-plane displacement components, ψ_x and ψ_y are the rotation components along the x and y axes, respectively. Substituting (2.15) through (2.17) into the small strain-displacement relations of elasticity theory yields :

$$\varepsilon_x = \frac{\partial u_o}{\partial x} + z\frac{\partial \psi_x}{\partial x} \qquad (2.18)$$

$$\varepsilon_y = \frac{\partial v_o}{\partial y} + z\frac{\partial \psi_y}{\partial y} \qquad (2.19)$$

$$\varepsilon_z = 0 \qquad (2.20)$$

$$\gamma_{xy} = \frac{\partial u_0}{\partial y} + \frac{\partial v_o}{\partial x} + z\left(\frac{\partial \psi_x}{\partial y} + \frac{\partial \psi_y}{\partial x}\right) \qquad (2.21)$$

$$\gamma_{xz} = \psi_x + \frac{\partial w}{\partial x} \qquad (2.22)$$

$$\gamma_{yz} = \psi_y + \frac{\partial w}{\partial y}\,. \qquad (2.23)$$

The stress strain relations for a orthotropic lamina, including the out of plane shear terms, are

$$\begin{bmatrix} \sigma_x \\ \sigma_y \\ \tau_{yz} \\ \tau_{xz} \\ \tau_{xy} \end{bmatrix} = \begin{bmatrix} Q_{11} & Q_{12} & 0 & 0 & Q_{16} \\ Q_{12} & Q_{22} & 0 & 0 & Q_{26} \\ 0 & 0 & Q_{44} & Q_{45} & 0 \\ 0 & 0 & Q_{45} & Q_{55} & 0 \\ Q_{16} & Q_{26} & 0 & 0 & Q_{66} \end{bmatrix} \begin{bmatrix} \varepsilon_x \\ \varepsilon_y \\ \gamma_{yz} \\ \gamma_{xz} \\ \gamma_{xy} \end{bmatrix}. \qquad (2.24)$$

Q_{ij} for i=1,2,6 are plane stress reduced stiffnesses, and Q_{ij} for i=4,5 are transverse shear stiffnesses. The force and moment resultants per unit length acting on the laminate are obtained by the integration of the stresses in each lamina through the plate thickness,

$$(Nx, Ny, Ny) = \int_{-h/2}^{h/2} (\sigma_x, \sigma_y, \tau_{xy}) dz \tag{2.25}$$

$$(Qx, Qy) = \int_{-h/2}^{h/2} (\tau_{xz}, \tau_{yz}) dz \tag{2.26}$$

$$(Mx, My, Mxy) = \int_{-h/2}^{h/2} (\sigma_x, \sigma_y, \tau_{xy}) z dz \tag{2.27}$$

Substituting equations (2.18-23) and (2.24) into equations (2.25-27) gives

$$\begin{bmatrix} N_x \\ N_y \\ Q_y \\ Q_x \\ N_{xy} \\ M_x \\ M_y \\ M_{xy} \end{bmatrix} = \begin{bmatrix} A_{11} & A_{12} & 0 & 0 & A_{16} & B_{11} & B_{12} & B_{16} \\ A_{12} & A_{22} & 0 & 0 & A_{26} & B_{12} & B_{22} & B_{26} \\ 0 & 0 & A_{44} & A_{45} & 0 & 0 & 0 & 0 \\ 0 & 0 & A_{45} & A_{55} & 0 & 0 & 0 & 0 \\ A_{16} & A_{26} & 0 & 0 & A_{66} & B_{16} & B_{26} & B_{66} \\ B_{11} & B_{12} & 0 & 0 & B_{16} & D_{11} & D_{12} & D_{16} \\ B_{12} & B_{22} & 0 & 0 & B_{26} & D_{12} & D_{22} & D_{26} \\ B_{16} & B_{26} & 0 & 0 & B_{66} & D_{16} & D_{26} & D_{66} \end{bmatrix} \begin{bmatrix} \frac{\partial u_o}{\partial x} \\ \frac{\partial v_o}{\partial y} \\ \frac{\partial w}{\partial y} + \psi_y \\ \frac{\partial w}{\partial x} + \psi_x \\ \frac{\partial u_o}{\partial y} + \frac{\partial v_o}{\partial x} \\ \frac{\partial \psi_x}{\partial x} \\ \frac{\partial \psi_y}{\partial y} \\ \frac{\partial \psi_x}{\partial y} + \frac{\partial \psi_y}{\partial x} \end{bmatrix}. \tag{2.28}$$

The extensional stiffness, Aij, coupling stiffness, Bij, and bending stiffness, Dij, are given by

$$(A_{ij}, B_{ij}, D_{ij}) = \int_{-h/2}^{h/2} (Q_{ij})_k (1, z, z^2) dz \qquad \text{i,j=1,2,6} \tag{2.29}$$

and

$$A_{ij} = K_i K_j \int_{-h/2}^{h/2} (Q_{ij})_k dz \qquad \text{i,j=4,5} \tag{2.30}$$

The shear correction factors are included to account for the fact that the transverse shear distributions are not uniform across the thickness of the plate.

Summing forces and moments on a differential element and neglecting the body forces, the equations of motion are reduced to:

$$\frac{\partial N_x}{\partial x}+\frac{\partial N_{xy}}{\partial y}=\rho^{\cdot}\frac{\partial^2 u_o}{\partial t^2}+R\frac{\partial^2 \psi_x}{\partial t^2} \tag{2.31}$$

$$\frac{\partial N_{xy}}{\partial x}+\frac{\partial N_y}{\partial y}=\rho^{\cdot}\frac{\partial^2 v_o}{\partial t^2}+R\frac{\partial^2 \psi_y}{\partial t^2} \tag{2.32}$$

$$\frac{\partial Q_x}{\partial x}+\frac{\partial Q_{xy}}{\partial y}=\rho^{\cdot}\frac{\partial^2 u_o}{\partial t^2} \tag{2.33}$$

$$\frac{\partial M_x}{\partial x}+\frac{\partial M_{xy}}{\partial y}-Q_x=R\frac{\partial^2 u_o}{\partial t^2}+I\frac{\partial^2 \psi_x}{\partial t^2} \tag{2.34}$$

$$\frac{\partial M_{xy}}{\partial x}+\frac{\partial M_y}{\partial y}-Q_y=R\frac{\partial^2 v_o}{\partial t^2}+I\frac{\partial^2 \psi_y}{\partial t^2}\ . \tag{2.35}$$

ρ is the mass density and

$$(\rho^{\cdot},R,I)=\int_{-h/2}^{h/2}\rho(1,z,z^2)dz. \tag{2.36}$$

By substituting equation (2.28) into equations (2.31-35), the equations of motion in terms of the displacements and rotation are obtained.

For this thesis, only symmetric laminates are considered. This results in considerable simplification because the coupling stiffnesses, Bij, and the normal-rotary inertia coupling coefficient ,R, are identically zero. The equations of motion for the flexural mode reduce to

$$A_{55}\left(\frac{\partial \psi_x}{\partial x}+\frac{\partial^2 w}{\partial x^2}\right)+A_{45}\left(\frac{\partial \psi_x}{\partial y}+\frac{\partial \psi_y}{\partial x}+2\frac{\partial^2 w}{\partial x\partial y}\right)+A_{44}\left(\frac{\partial \psi_y}{\partial y}+\frac{\partial^2 w}{\partial y^2}\right)=\rho^{\cdot}\frac{\partial^2 w}{\partial t^2} \tag{2.37}$$

$$D_{16}\frac{\partial^2 \psi_x}{\partial x^2}+(D_{12}+D_{66})\frac{\partial^2 \psi_x}{\partial x\partial y}+D_{26}\frac{\partial^2 \psi_x}{\partial y^2}+D_{66}\frac{\partial^2 \psi_y}{\partial x^2}+2D_{26}\frac{\partial^2 \psi_y}{\partial x\partial y}$$
$$-A_{44}\left(\psi_y+\frac{\partial w}{\partial y}\right)=I\frac{\partial^2 \psi_y}{\partial t^2}\ . \tag{2.38}$$

$$D_{11}\frac{\partial^2\psi_x}{\partial x^2}+2D_{16}\frac{\partial^2\psi_x}{\partial x\partial y}+D_{16}\frac{\partial^2\psi_x}{\partial x^2}+(D_{12}+D_{66})\frac{\partial^2\psi_y}{\partial x\partial y}+D_{26}\frac{\partial^2\psi_y}{\partial y^2}-A_{55}(\psi_x+\frac{\partial w}{\partial x})$$
$$-A_{45}(\psi_y+\frac{\partial w}{\partial y})=I\frac{\partial^2\psi_x}{\partial t^2}. \qquad (2.39)$$

For flexural wave propagation , we consider plane waves described by

$$w = We^{i(k(l_1x+l_2y)-\omega t)} \qquad (2.40)$$

$$\psi_x = \psi_x e^{i(k(l_1x+l_2y)-\omega t)} \qquad (2.41)$$

$$\psi_y = \psi_y e^{i(k(l_1x+l_2y)-\omega t)}. \qquad (2.42)$$

The value k is the wave number, l1 and l2 are the direction cosines of the wave vector in the x and y directions, ω is the circular frequency, and W, ψ_x and ψ_y are the amplitudes of the plane waves. After substituting equations (2.40- 42) into equations (2.37 - 39), the determinant of the resulting set of equations gives the dispersion (characteristic) equation for flexural wave propagation. Because this study is limited to symmetric quasi-isotropic laminates, in addition to B_{ij} and R=0, $A_{16} = A_{26} = A_{45} = 0$ and $D_{16} = D_{26}$. This results in the following characteristic equation for flexural wave propagation.

$$\begin{bmatrix} D_{11}K^2l_1^2+2D_{16}k^2l_1l_2 & D_{16}k^2+(D_{12}+D_{66})K^2l_1l_2 & iA_{55}kl_1 \\ +D_{66}K^2l_2^2+A_{55}-I\omega^2 & & \\ D_{16}k^2+(D_{12}+D_{66})k^2l_1l_2 & D_{66}k^2l_1^2+2D_{16}K^2l_1l_2 & iA_{44}kl_2 \\ & +D_{22}k^2l_2+A_{44}-I\omega^2 & \\ -iA_{55}kl_1 & -iA_{44}kl_2 & -A_{55}k^2l_1^2-A_{44}k^2l_2^2-\rho\dot{}\omega^2 \end{bmatrix} = 0 \qquad (2.43)$$

Several simplifications can be made for waves propagating along principal directions. For waves propagating in the x- direction (l_1=1 and l_2=0),equation (2.43) reduces to

$$(D_{11}k^2 + A_{55} - I\omega^2)(D_{66}k^2 + A_{44} - I\omega^2)(A_{55}k^2 - \rho^{\cdot}\omega^2)$$

$$-(D_{16}k^2)^2(A_{55}k^2 - \rho^{\cdot}\omega^{22}) - (A_{55}k)^2(D_{66}k^2 + A_{44} - I\omega^2) = 0 \ . \qquad (2.44)$$

For waves propagating in the y-direction, equation (2.43) reduces to

$$(D_{22}k^2 + A_{44} - I\omega^2)(D_{66}k^2 + A_{55} - I\omega^2)(A_{44}k^2 - \rho^{\cdot}\omega^2)$$

$$-(D_{16}k^2)^2(A_{44}k^2 - \rho^{\cdot}\omega^{22}) - (A_{44}k)^2(D_{66}k^2 + A_{44} - I\omega^2) = 0 \qquad (2.45)$$

For unidirectional or cross-ply laminates, equation (2.43) can be further simplified (since $D_{16}=0$) for waves propagating in principal directions. For waves propagating in the x-direction (2.44) reduces to

$$(D_{11}k^2 + A_{55} - I\omega^2)(A_{55}k^2 - \rho^{\cdot}\omega^2) - A_{55}{}^2k^2 = 0$$

(2.46)

For waves propagating in the y-direction (3.45) reduces to

$$(D_{22}k^2 + A_{44} - I\omega^2)(A_{44}k^2 - \rho^{\cdot}\omega^2) - A_{44}{}^2k^2 = 0$$

(2.47)

It can be recognized that the characteristic equation has more than one root. However, only one root approaches zero circular frequency as the wave number approaches zero. This is the root corresponding to the flexural branch of the frequency spectrum for plate waves.

III. DISPERSION MEASUREMENTS

A. INSTRUMENTATION AND EXPERIMENTAL PROCEDURE

Figure 3.1 is a schematic of the instrumentation used for the phase velocity measurements. An arbitrary function generator (AFG), (LeCroy model 9100) was used to generate a 10 volt, peak-to-peak, gated nine cycle sine wave tone burst, shown in figure 3.2. The repetition rate of the tone burst was controlled by a 20 MHz pulse generator (Wavetek model 145). The tone burst from the AFG was amplified using a direct coupled amplifier (Krohn-Hite model DCA-50) over the frequency range of 0-500 kHz. The amplified signal was in turn input into a matching transformer (Khron-Hite model MT-55). The signal was used to drive a piezoelectric transducer which was used to transmit the wave into the plate. Several different transmitter and receiver transducer types were used to increase the size of the flexural mode. This issue is discussed in depth in section C of this chapter. Both exciter and receiver transducers were coupled to the plate using vacuum grease. The received signal was then amplified 60 dB using a model 1220A Physical Acoustics Corporation (PAC) preamplifier , in which the filter had been modified for broadband operation. Finally, the output signal was routed to a LeCroy 9400A digital oscilloscope to capture and digitize the waveform detected by the receiving transducer.

In order to measure the phase velocity, a cursor on the oscilloscope screen was positioned at a reference point on the received wave. The receiving transducer was then moved a known distance, l. By maintaining the cursor at the reference point (phase point) of the waveform as the receiving transducer was translated, the time difference , Δt, of the phase point was determined. Knowing

the time difference and the distance of transducer travel, it is a simple calculation to determine the phase velocity, $Vp=l/\Delta t$.

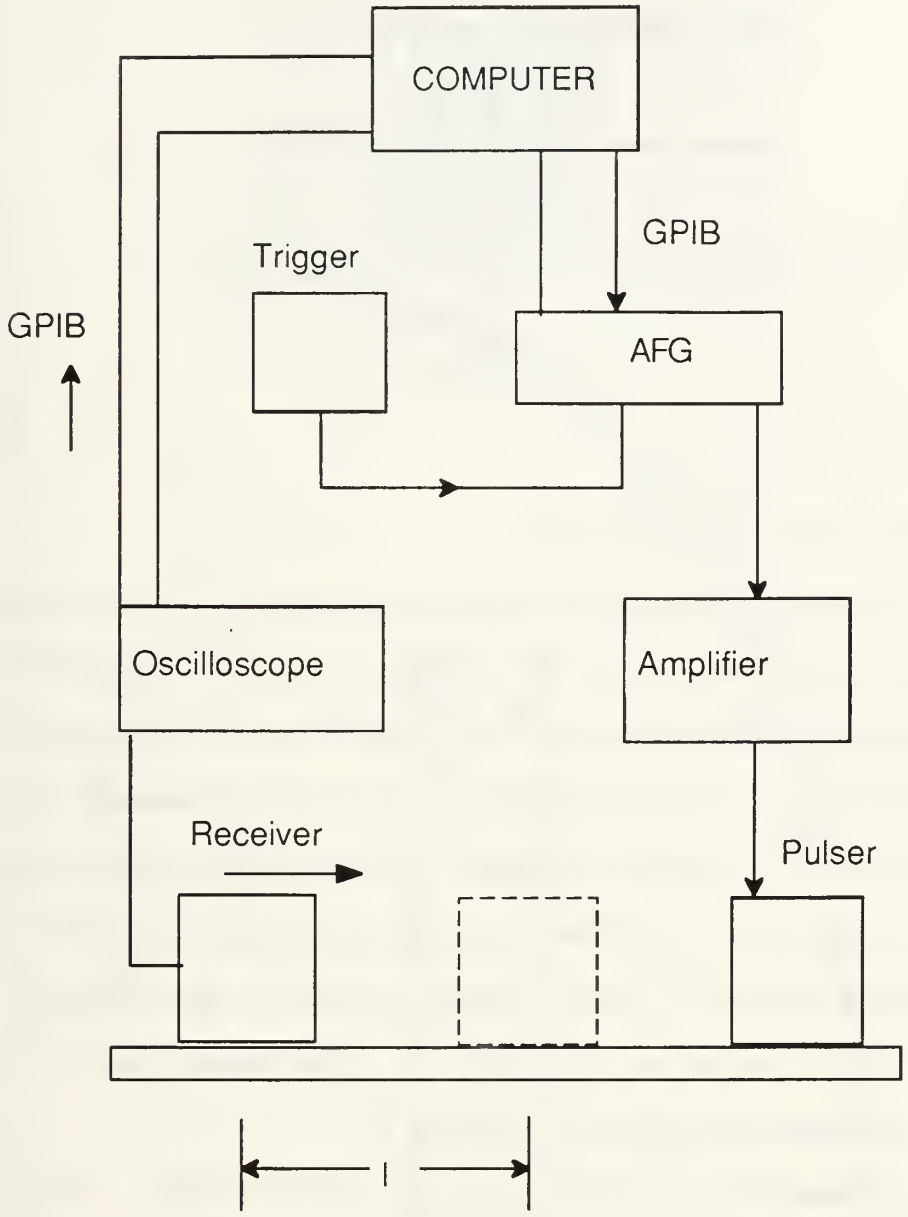

Figure 3.1 Schematic of Experimental Set-up

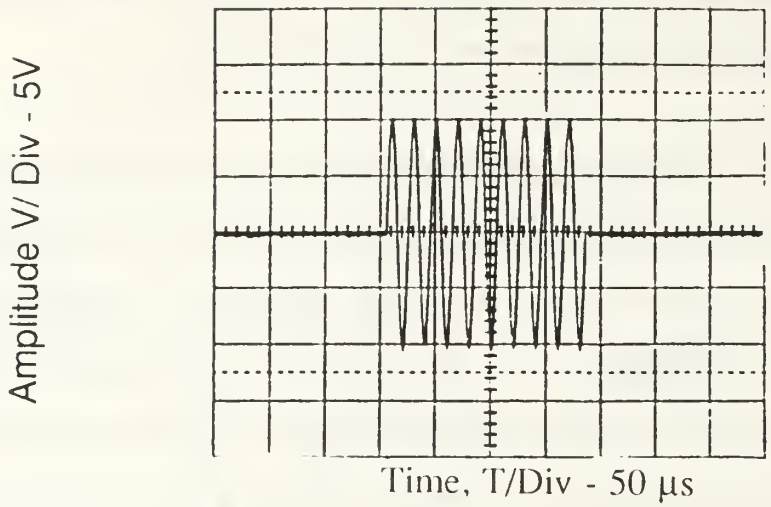

Figure 3.2 Input pulse

B. EXPERIMENTAL RESULTS

Shown in Figures 3.3 and 3.4 are the theoretical dispersion curves (from higher order plate theory) for the $[0,90]_{4,S}$ laminate. Additionally, the experimental phase velocities are shown for the flexural waves propagating in the 0 and 90 degree directions. Figures 3.5 to 3.9 are the theoretical dispersion curves for the $[0,45,90,-45]_{2,s}$ laminate. The experimentally derived phase velocities are shown for the flexural waves propagating in the 0, 22.5, 45, 67.5 and 90 degree direction. Material constants used for the calculation of the dispersion curves are given in Appendix A. Experimental data for all phase velocity measurements are given in Appendix B.

The experimental data follows the general trend of theory. Except for the $[0,90]_{4,S}$ laminate measured in the 0° direction, the experimental phase velocities are consistently less than the theoretical. It is believed that this discrepancy is due to the actual elastic constants being less than those quoted by the manufacturer.

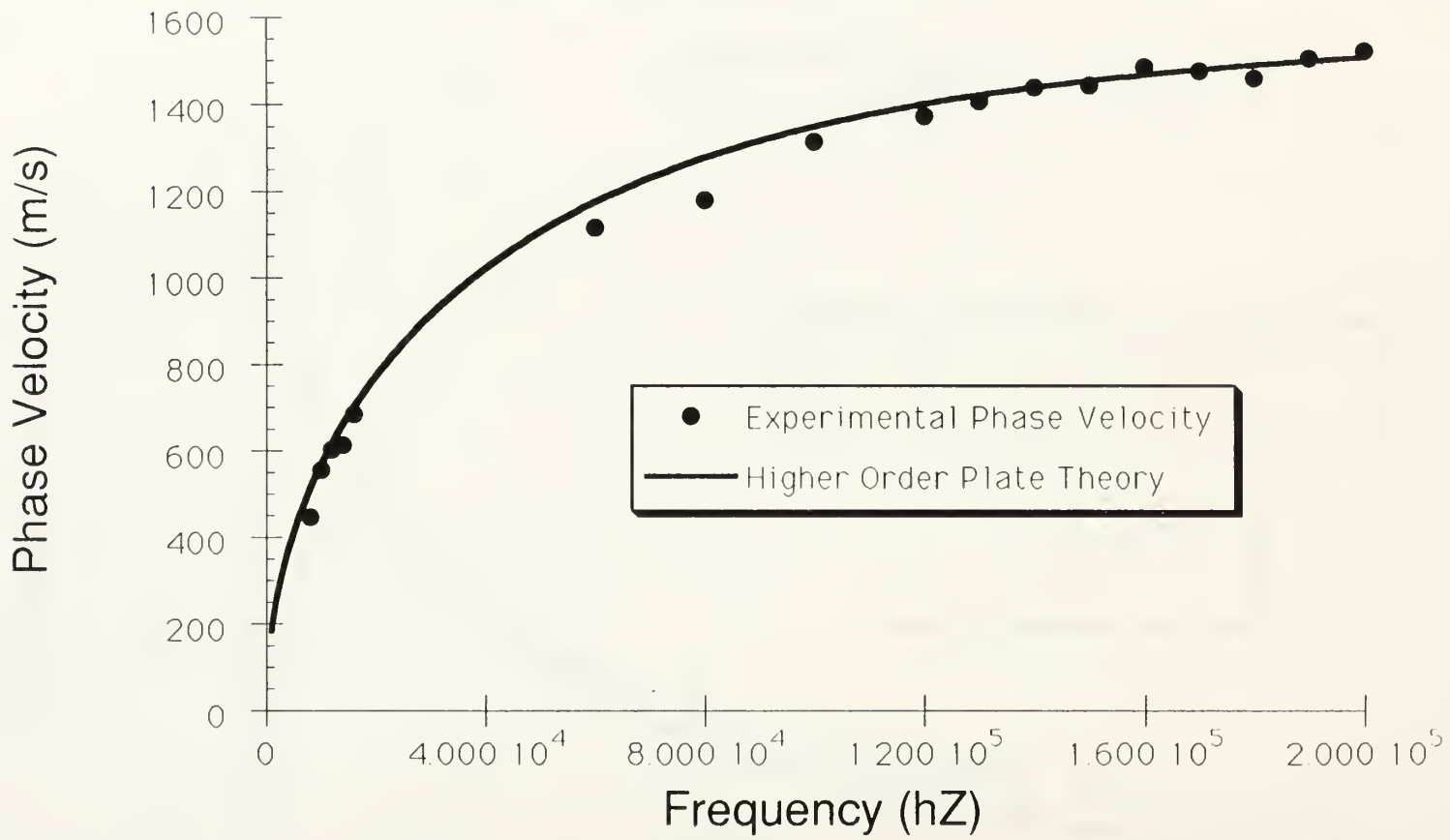

Figure 3.3 Theoretical Dispersion curves and data for $[0,90]_{4,S}$, 0° direction

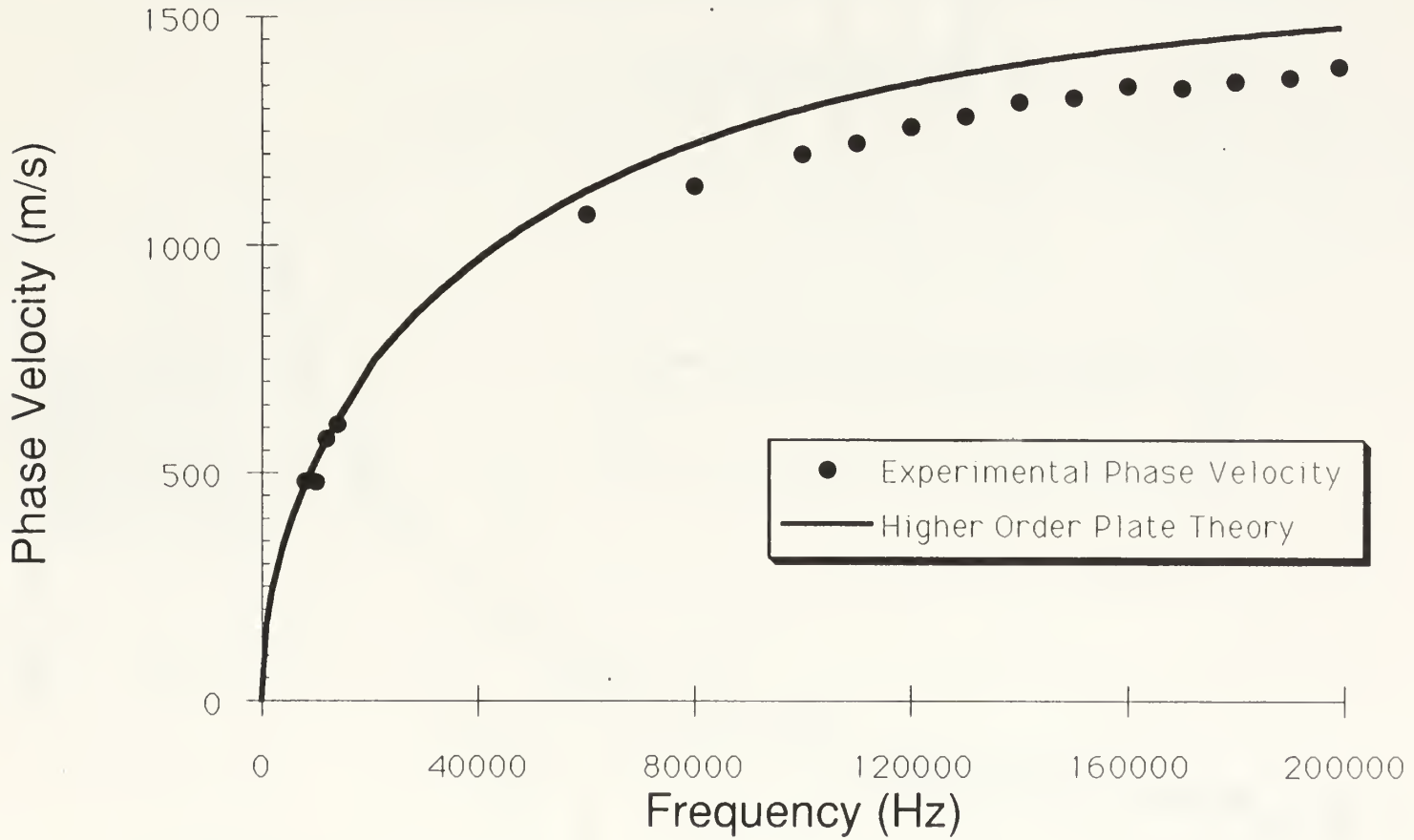

Figure 3.4 Theoretical Dispersion curves and data for $[0,90]_{4,S}$, 90° direction

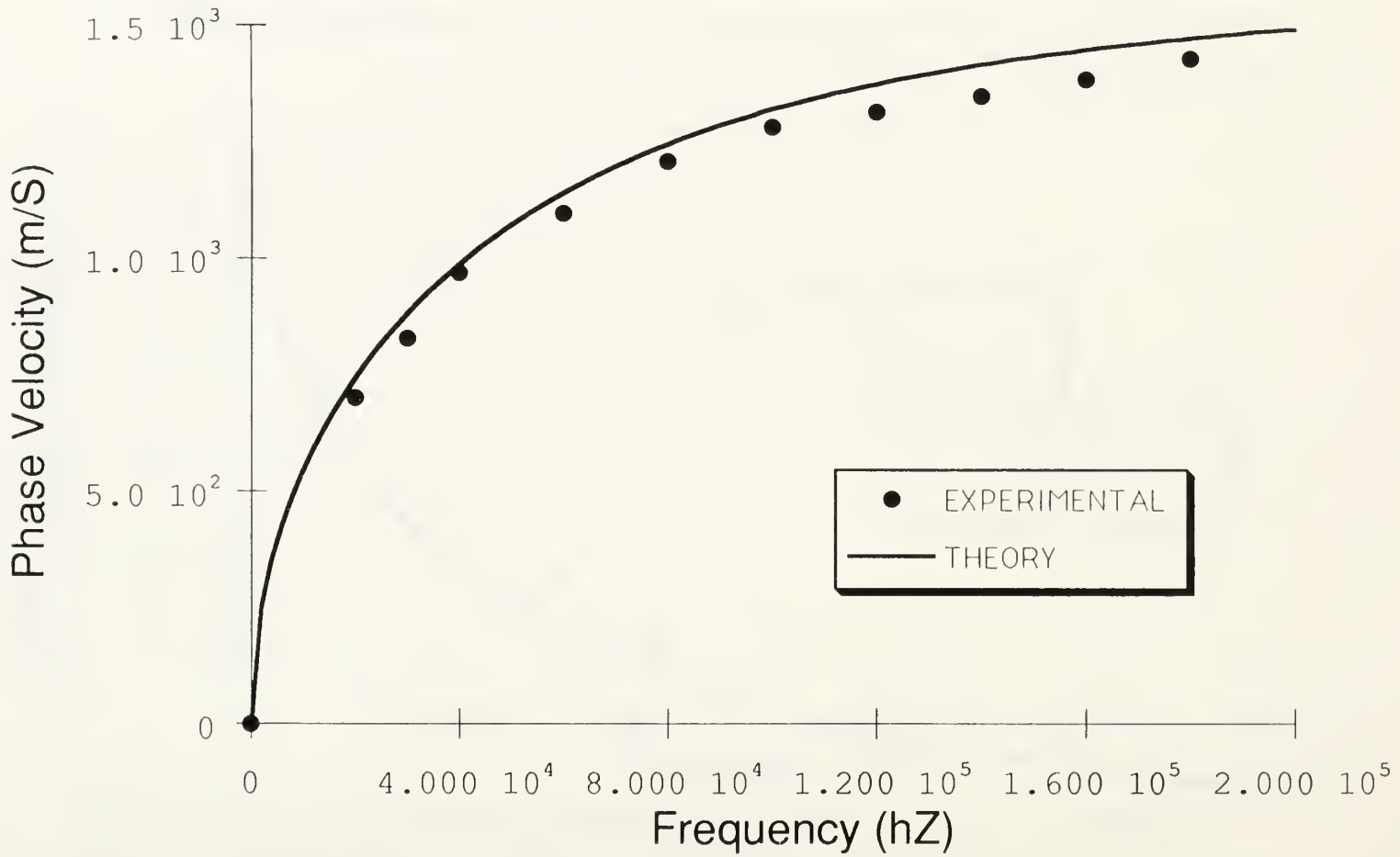

Figure 3.5 Theoretical Dispersion curves and data for $[0,45,90,-45]_{2,S}$, 0° direction

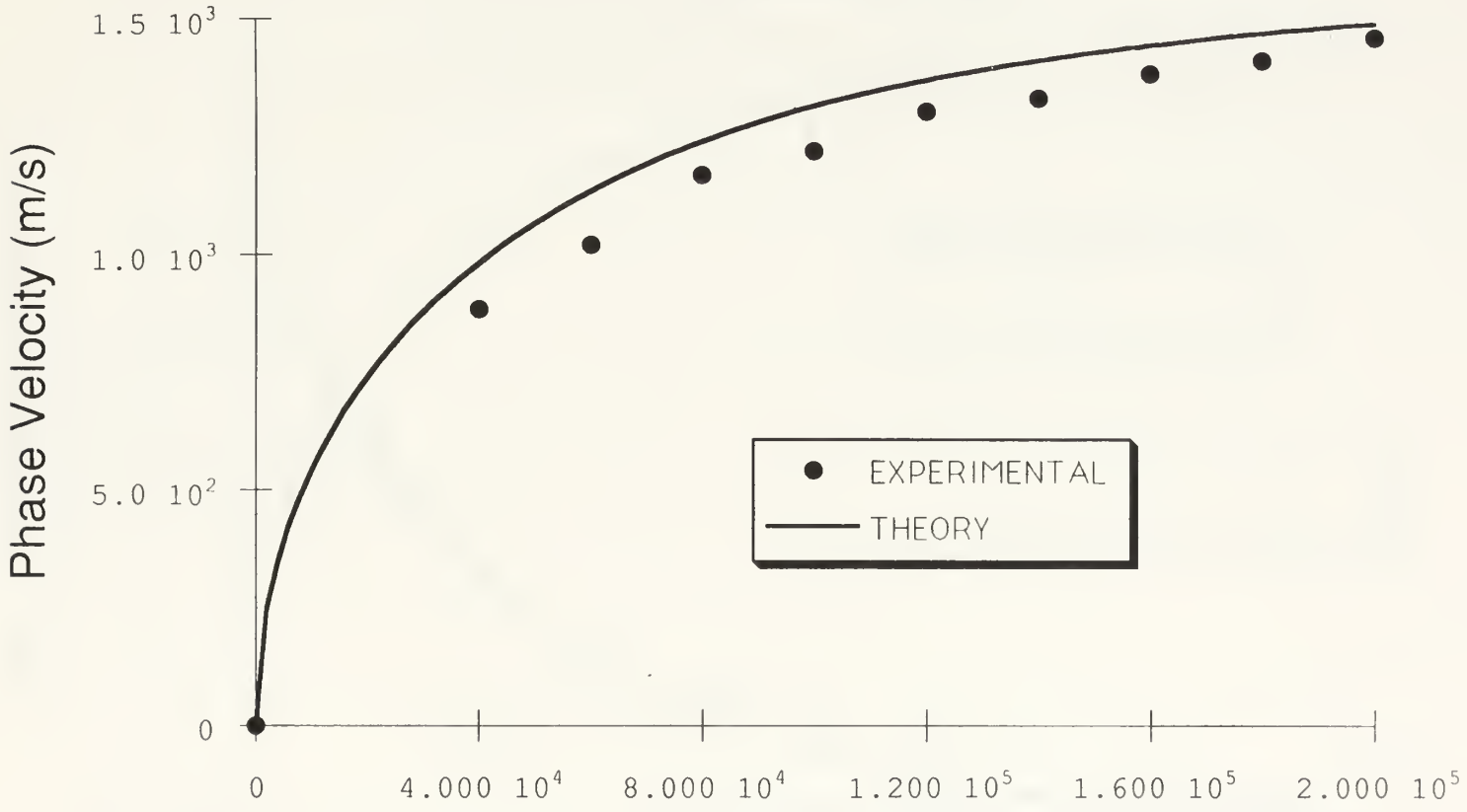

Figure 3.6 Theoretical Dispersion curves and data for [0,45,90,-45] $_{2,S}$, 225° direction

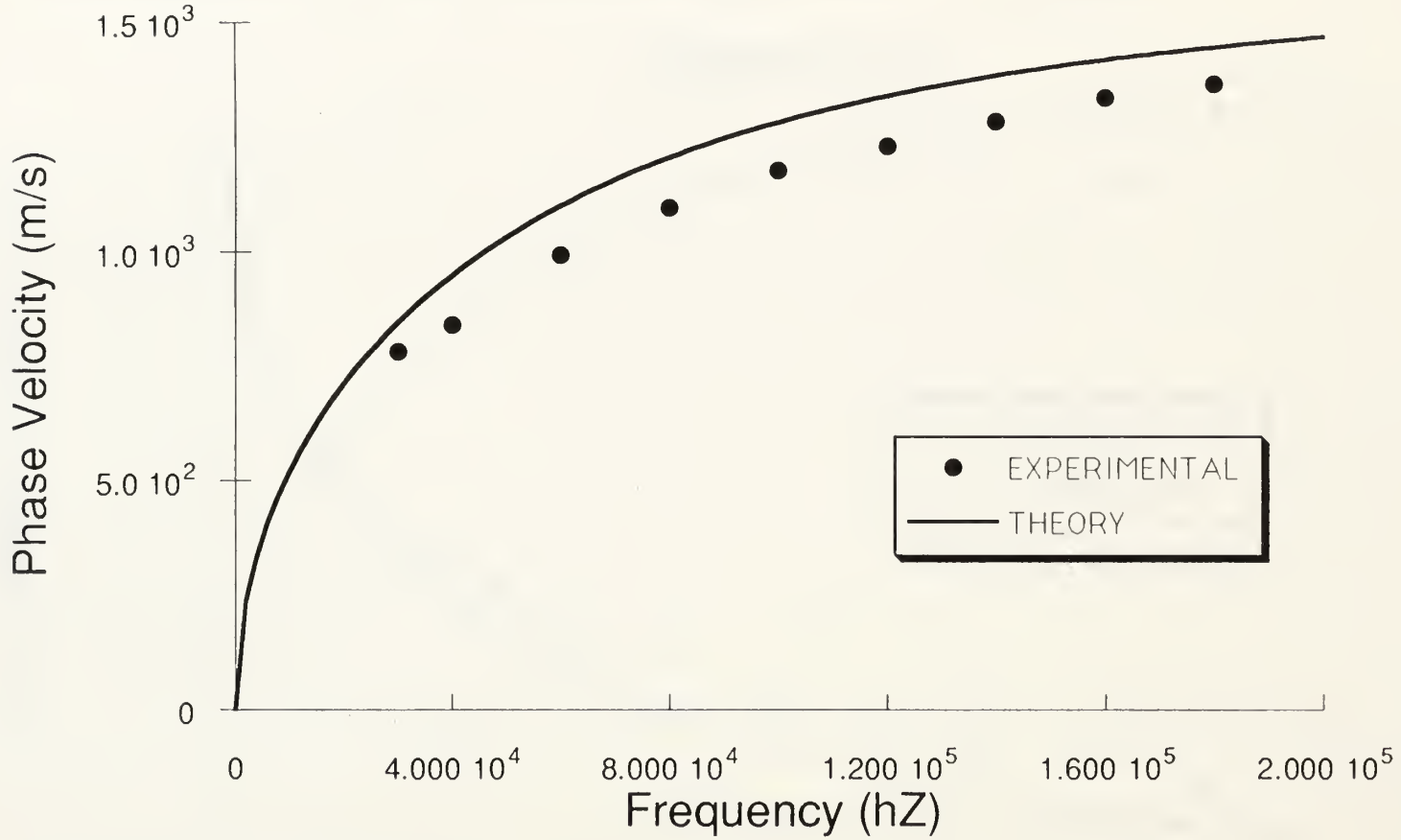

Figure 3.7 Theoretical Dispersion curves and data for [0,45,90,-45] $_{2,S}$, 45° direction

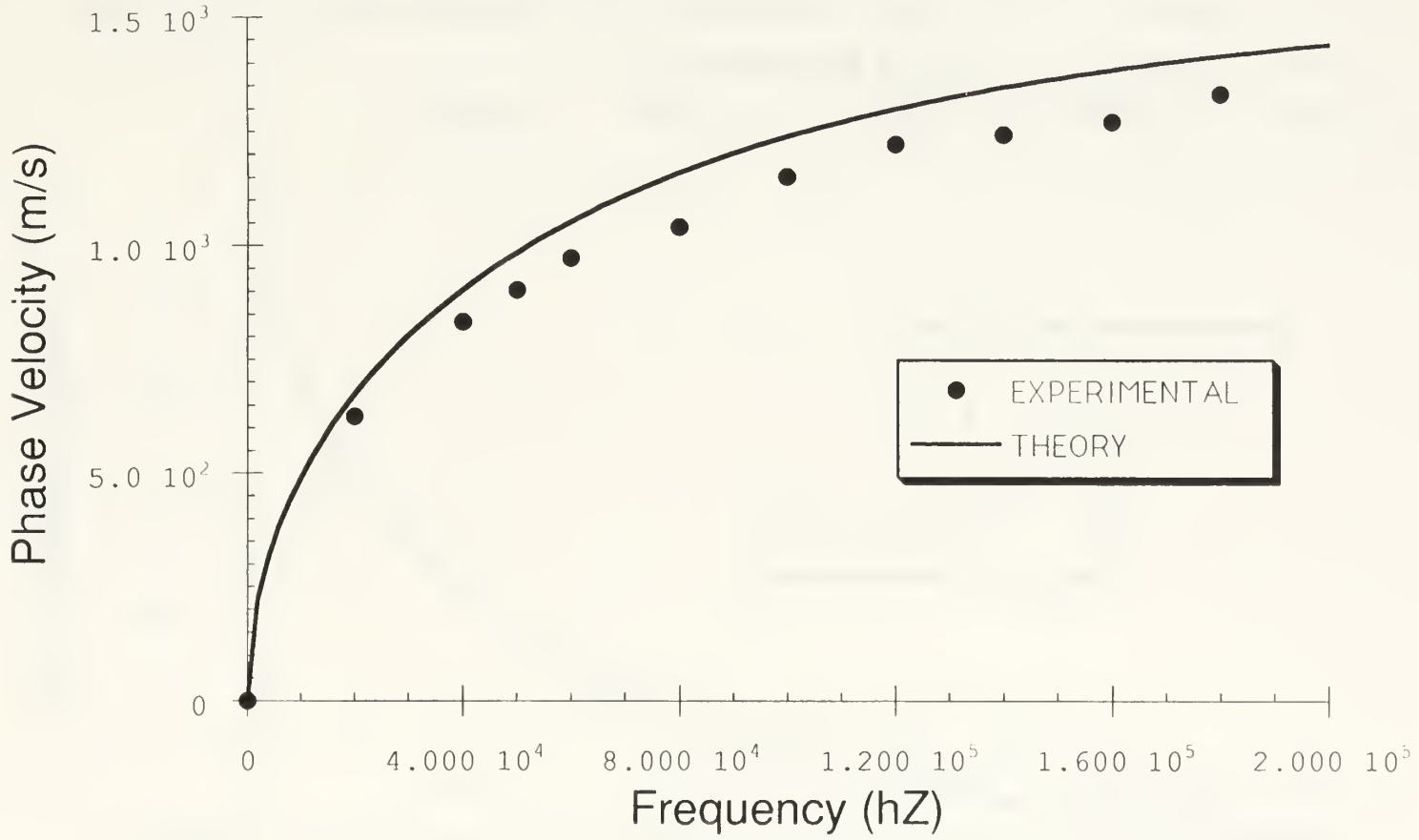

Figure 3.8 Theoretical Dispersion curves and data for [0,45,90,-45]$_{2,S}$, 67.5° direction

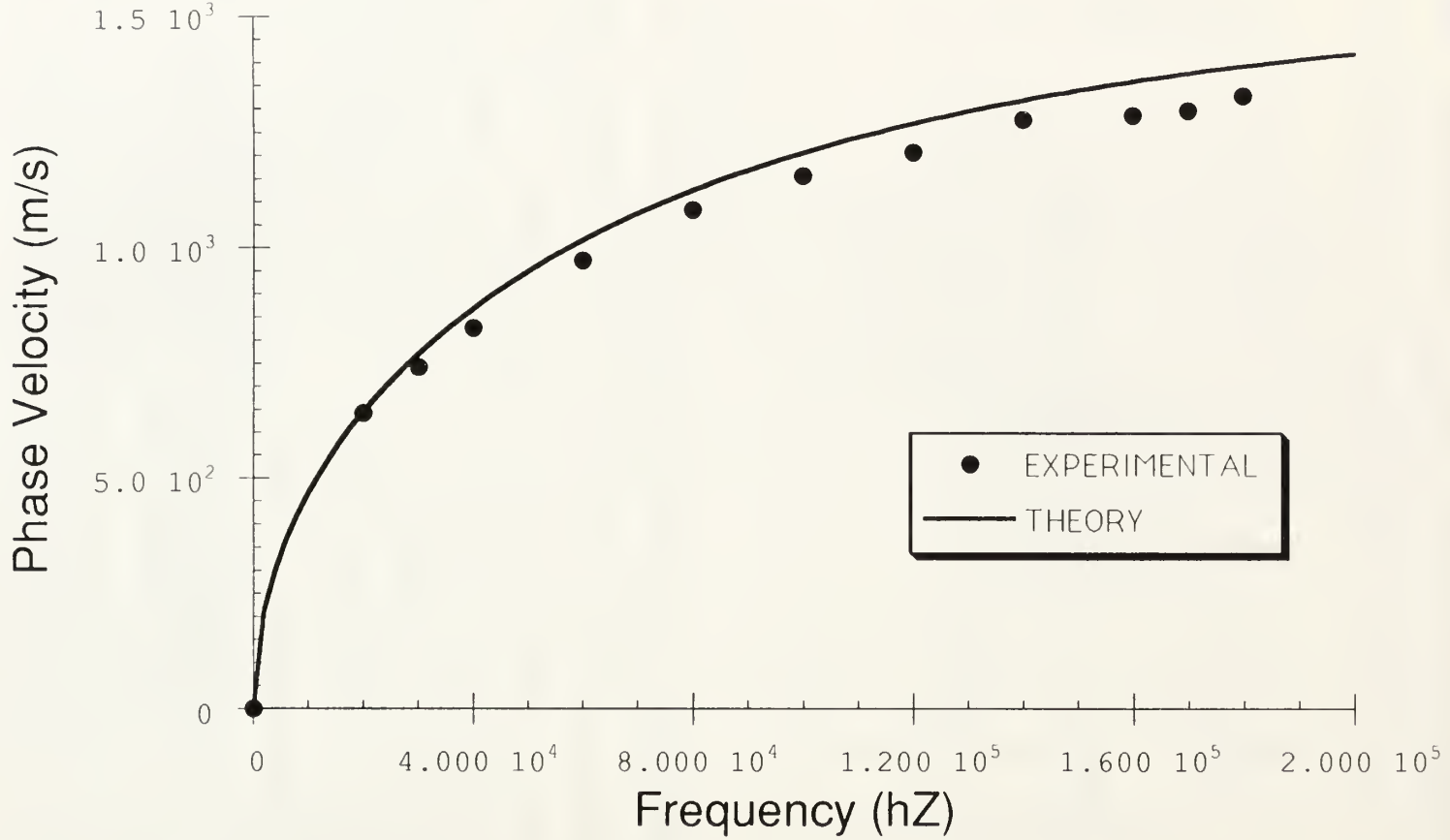

Figure 3.9 Theoretical Dispersion curves and data for [0,45,90,-45] $_{2,S}$, 90° direction

Several subtleties associated with experimental phase velocity measurements were discovered which are discussed below.

The selection of the transducer (size and resonant frequency) pulser/ receiver combination had an important result on the mode of the output wave. For example, when measuring the [0,90]4,s plate at the lower frequencies the combination of transducer A/B (as defined in Appendix B) produced an excellent presentation of the flexural mode (Figure 3.10). As the frequency is increased the extensional mode is introduced into the laminate (Figure 3.11). By switching the pulser/ receiver combination to B/C, the effect of the extensional mode is decreased (Figure 3.12). This may be due to the smaller diameter transducers not being excited by the extensional mode at this frequency. This is because the wavelength was much larger than the transducer diameter. The separation of the flexural and extensional mode ensured that the proper flexural mode was utilized to measure the phase velocity.

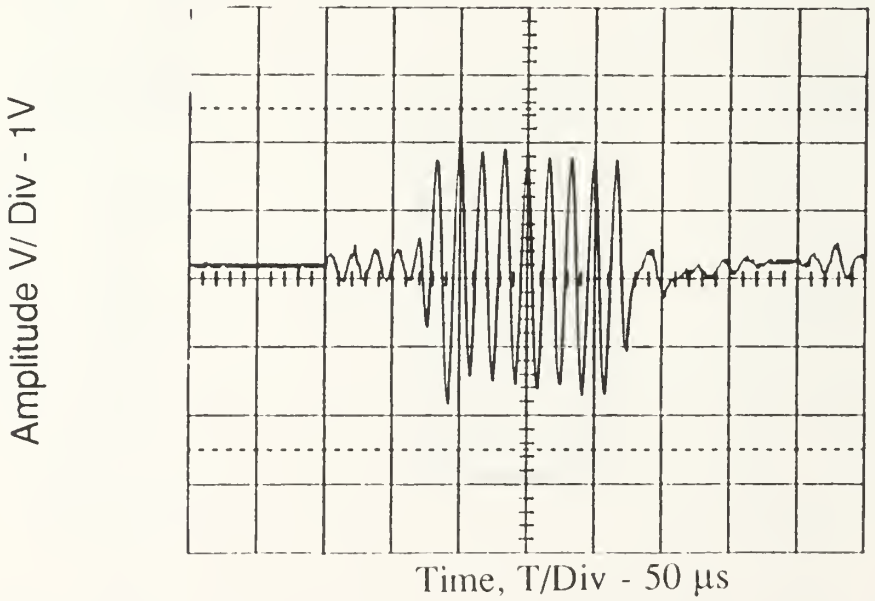

Figure 3.10 Reference wave form , $[0,90]_{4,s}$ laminate, (frequency= 60kHz)

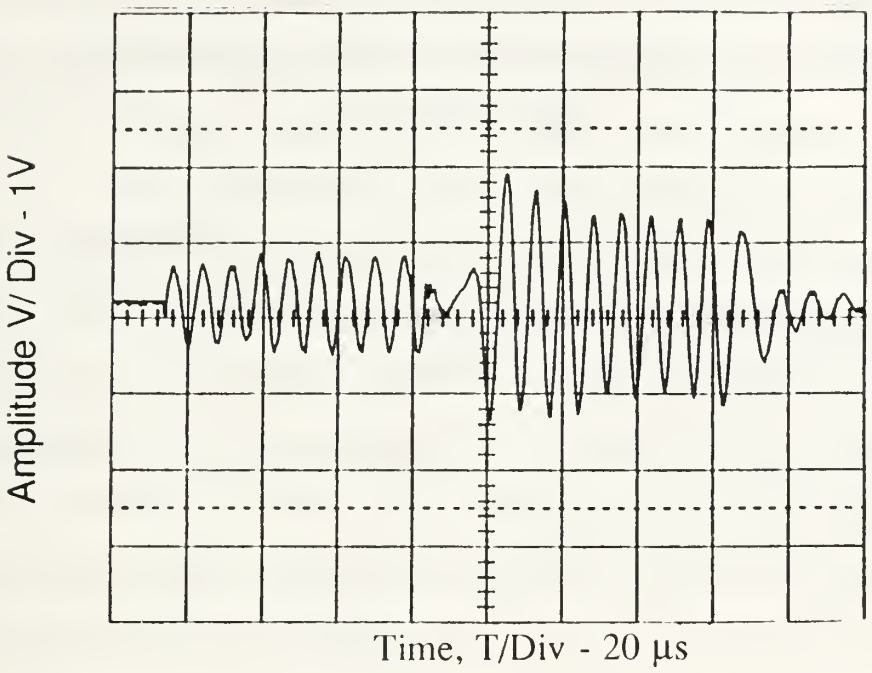

Figure 3.11 Extensional and flexural wave excitation, $[0,90]_{4,s}$ laminate, (frequency= 130 kHz), A/B Transducer Combination

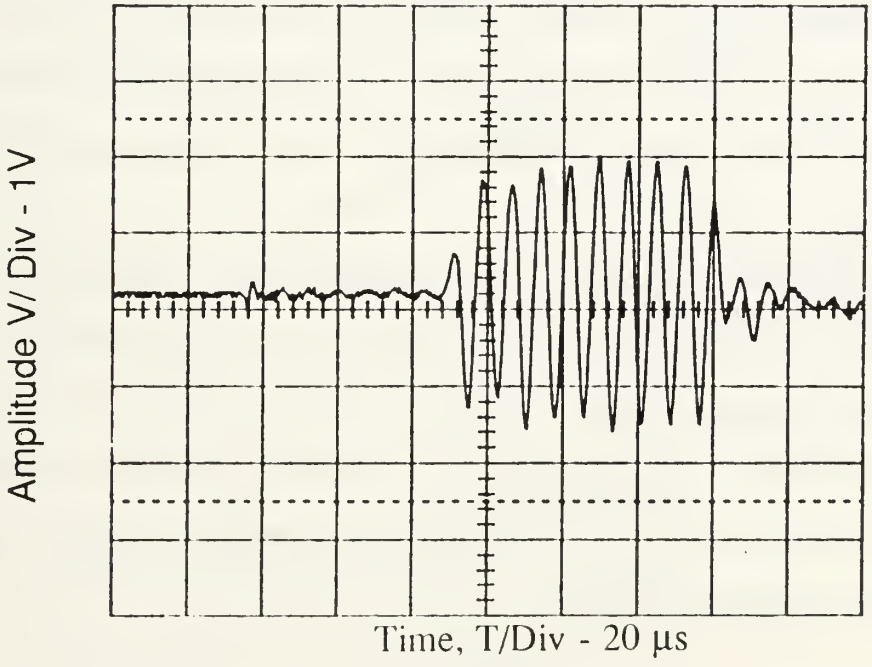

Figure 3.12 Delay of extensional mode due to transducer switch, [0,90]4,s laminate ,130 kHz, B/C transducer combination.

Delaying the onset of the extensional mode relative to the flexural mode was also important to eliminate the problem of the extensional mode mixing and interfering with the flexural mode. This is a significant problem because if the two modes mix an incorrect phase velocity would be measured.

The upper limit of flexural mode phase velocity measurements was realized when the extensional mode interfered and overpowered the flexural modes. For the [0,90]4,s plate this occurred at 220 kHz in the 90° direction and 260 kHz in the 0° direction. For the $[0,45,90,-45]_{2,s}$ laminate the upper limit was generally realized at 200 kHz for all directions.

Because the experimental laminates were of finite lengths, wave reflections at certain frequencies were of concern. The mixing of the signal and reflections could produce an erroneous phase velocity. Because it was not possible to cancel all reflections, some frequencies were not measured due to this phenomenon.

In summary, the experimental measurements of phase velocity required an understanding of the wave propagation. It was imperative to differentiate between the flexural and extensional modes and to realize the effects of the reflections.

The first aspect of this thesis was concerned with verifying the higher order plate theory by comparing experimentally measured phase velocities to theoretically determined phase velocities. The second aspect of this thesis will now be concerned with using the experimental phase velocities to determine the laminate material properties by inverting the governing equations. This will be discussed in the following section.

IV. ALGORITHMS FOR RECOVERING MATERIAL CONSTANTS

A. $[0]_{16}$ LAMINATE

Figure 4.1 is a comparison of dispersion curves using both classical plate theory (CPT) and higher order plate theory (HOPT) for the $[0]_{16}$ laminate. There is agreement, within a 5% variation, between the two theories if the frequency is limited to 19.0 kHz. At frequencies higher than 19.0 kHz, greater error arises in the phase velocities predicted by CPT due mainly to neglecting the shear deformation and rotary inertia.

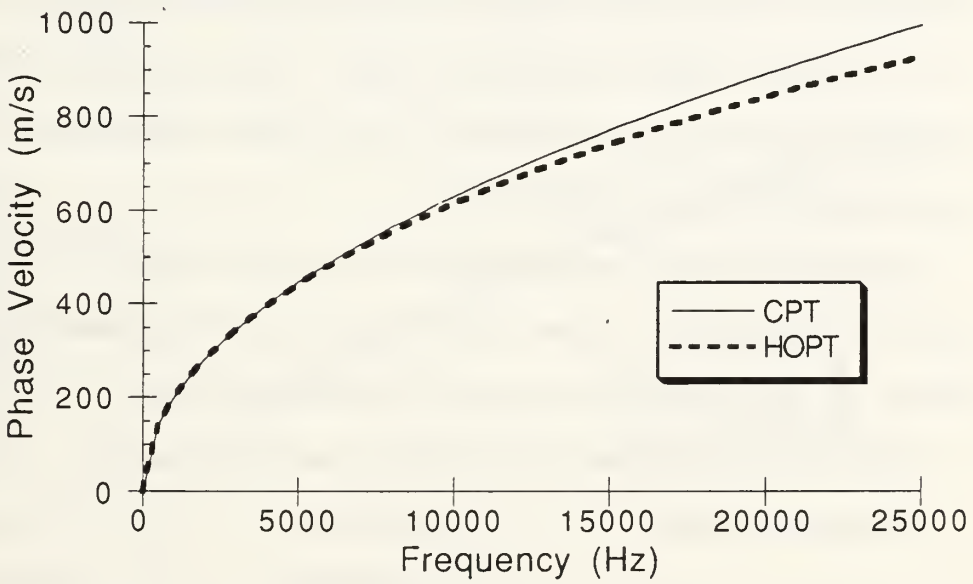

Figure 4.1 CPT vs. HOPT $[0]_{16}$ laminate , 0° direction.

Rearranging equation (2.13) to solve for D_{11} yields

$$D_{11} = \left(\frac{V_p^4 \rho h}{4\pi^2 f^2}\right). \qquad (4.1)$$

Consequently, by using classical plate theory at the lower frequency regime, it is possible to recover D_{11} by measuring the experimental phase velocity along the x-direction. The experimental frequency, plate thickness and plate density are known. Table 4.1 is a comparison of experimental values of D_{11} against the theoretical values. Classical lamination theory, which assumes static loading, was used to calculate D_{11}. All experimental numbers used in the calculations of material properties were described in the previous chapter.

Different frequencies were investigated to determine the effect of frequency on the material properties. The experimental error at 6 kHz was greater due to higher uncertainties when measuring the time differences due to lower signal to noise ratios, excitation of the transducer's resonant frequency and reflections. These phenomena are discussed in more detail at the end of this section. From analyzing the 8 kHz and the 10 kHz measurements, the values for D_{11} were found to be consistent within experimental error. Further analysis should include multiple experimental measurements at the same frequency to differentiate between systematic and random errors.

Experimental errors were determined from procedures set forth by Holman [Ref. 15]. Appendix C shows all calculations and experimental uncertainties used for the determination of the total experimental error.

Table 4.1 $[0]_{16}$ laminate, Experimental and theoretical D_{11}

Frequency (kHz)	D_{11} (Nm) (Experimental)	D_{11} (Nm) (Laminate Plate Theory)
6.0	148.1 (+/- 9.62)	140.0
8.0	120.1 (+/- 8.26)	140.0

10.0	122.7 (+/- 8.87)	140.0

The discrepancy between experimental results and laminate plate theory is most likely due to the typical material constants supplied by the manufacturer being greater than the "as-manufactured" material constants of this particular plate. An area for further analysis would be to compare acoustically measured material properties to those derived from mechanical tests of specimens from the experimental laminates.

Figure 4.2 is a graphical comparison of dispersion curves using CPT and HOPT of the $[0]_{16}$ laminate for waves propagating in the 90 degree direction.

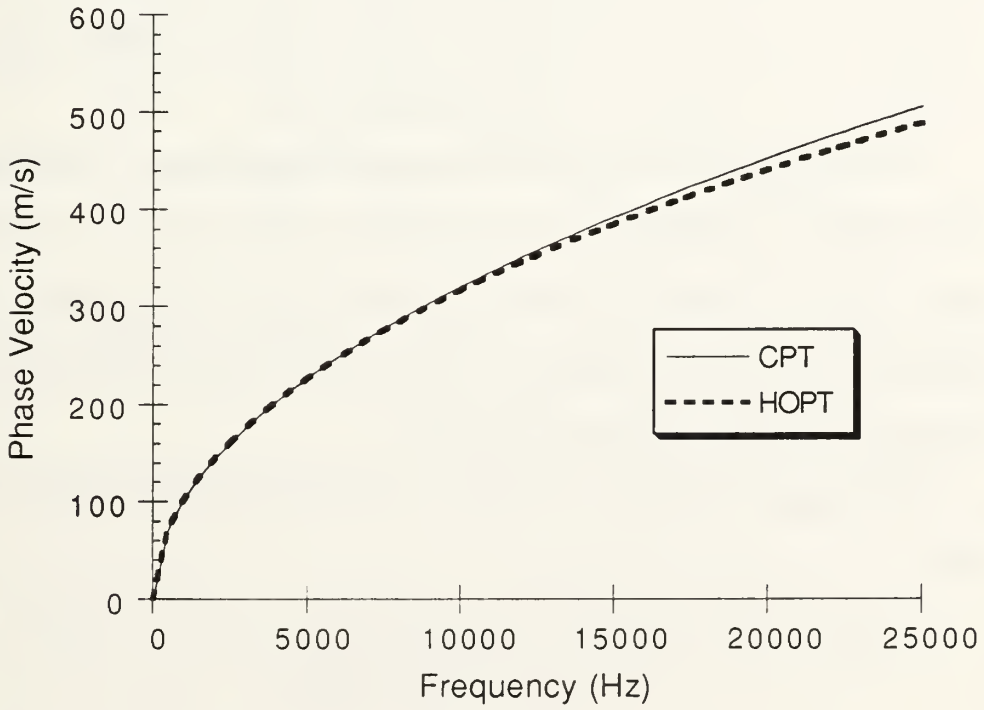

Figure 4.2 CPT vs. HOPT $[0]_{16}$ laminate , 90° direction

Rearranging equation (2.14) to solve for D_{22} yields

$$D_{22} = \left(\frac{V_p^4 \rho h}{4\pi^2 f^2}\right). \qquad (4.2)$$

when measuring phase velocities of flexural waves propagating in the y-direction.

As before in the x-direction, by limiting experimental frequencies to the regions where classical plate theory and higher order plate theory agree, it was possible to use CPT to recover D_{22}. Table 4.2 is a comparison of experimental D_{22} against the theoretical D_{22} .

Table 4.2 $[0]_{16}$ laminate Experimental and Theoretical D_{22}

Frequency (kHz)	D_{22} (Nm) (experimental)	D_{22} (Nm) (plate theory)
6.0	10.4 (+/- 1.38)	9.35
8.0	13.2 (+/- 2.0)	9.35
10.0	12.2 (+/- 1.97)	9.35

The experimental results are within experimental error of each other but the 8 and 10 kHz measurements were not within experimental error of laminate plate theory. Again, an area for further analysis would be to compare acoustically measured material properties to those derived from mechanical tests of specimens from the experimental laminate.

All remaining material properties were calculated using higher order plate theory.

Equation (2.46) algebraically rearranged to solve for A_{55} yields

$$A_{55} = \frac{\rho^{\cdot}\omega^2(D_{11}k^2 - I\omega^2)}{D_{11}k^4 - \rho^{\cdot}\omega^2 - I\omega^2 k^2}. \qquad (4.3)$$

Likewise, equation (2.47) algebraically rearranged to solve for A_{44} yields

$$A_{44} = \frac{\rho \omega^2 (D_{22} k^2 - I\omega^2)}{D_{22} k^4 - \rho \omega^2 - I\omega^2 k^2}. \qquad (4.4)$$

The first attempt at solving A_{44} and A_{55} was made using the lower frequencies and phase velocities used to calculate D_{11} and D_{22}. This first attempt yielded negative values of A_{44} and A_{55} which was obviously an erroneous result. This error was due to the fact that (4.3) and (4.4) are quadratic equations with more than one root. The experimental frequency was increased to excite the positive root of A_{44}. Since this was only a quick check of an algorithm to recover material constants, only A_{44} was investigated for an experimental recovery. The frequency was increased to 100 kHz and the subsequent measured phase velocity resulted in an A_{44} of 5.38 MPa which compares favorably, within experimental error, to the theoretical value of 6.78 Mpa.

Since $D_{16} = 0$ for a unidirectional plate, the following equation can be factored from equation (3.44):

$$D_{66} k^2 + A_{44} - I\omega^2 = 0. \qquad (4.5)$$

Equation (5.5) rearranged to solve for D66 gives

$$D_{66} = \frac{I\omega^2 - A_{44}}{k^2}. \qquad (4.6)$$

This is a quadratic equation in terms of the frequency. Recovering the positive root of this equation dictated the experimental frequency be increased to over 300 kHz. This presented a serious problem since in this frequency regime the extensional mode dominates, making the experimental measurement of the flexural mode impossible. Consequently, it was not possible to recover D_{66} and ultimately D_{12}. D_{12} was to be calculated by equation (2.43) when measuring phase velocities in off-principal directions with all other material properties known.

In summary, by restricting the experimental frequency to the regime where CPT and HOPT agree, values of D_{11} and D_{22} were recovered from CPT. However, measuring at these lower regimes presented their own problems and errors and was found to be difficult. The transducers used were not very sensitive at these lower frequencies resulting in low signal to noise ratios. The unidirectional laminate was especially prone to reflections when measuring in the 90 degree direction. The waves propagated significantly faster in the 0 degree direction than in 90 degree direction. Consequently, when measuring in the 90° direction, the reflections of waves propagating in the 0° direction interfered with the direct wave propagation along the 90°direction likewise making measurements difficult. The PAC R15 transducer was utilized for measurements in the 0° direction. When measurements were accomplished with the PAC R15, higher frequencies were introduced due to the input gated sine wave. The higher frequencies excited the transducer's resonant frequency which "rode" on top of the input frequency making measurements difficult.

B. $[0,45,90,-45]_{2,S}$ LAMINATE

While employing classical plate theory for the recovery of D_{11} and D_{22} for the unidirectional plate was successful, the inability to recover D_{12} and D_{66} dictated the use of a more powerful algorithm. For the $[0,45,90,-45]_{2,s}$ laminate, it was not possible to calculate A_{44} and A_{55} directly as before because D_{16} was no longer zero. It was determined that a desirable algorithm would be based upon equation (2.44). By assuming wave propagation along principal directions (0 or 90 degrees) a significant simplification of the governing equation results. By successfully incorporating classical plate theory to determine D_{11} and D_{22}, the unknown material properties in (2.44) were reduced to 4 (A_{44}, A_{55}, D_{16} and

D_{66}). Once these unknowns were accounted for, it would then be possible to determine D_{12} from equation (2.43).

CPT and HOPT agree within 5% if the experimental frequency is limited to 16.5 kHz when measuring in the 0° direction (Figure 4.3). Equation (4.1) was applied to recover D_{11} when limiting the experimental frequency to less than 16.5 kHz. Table 4.3 is presented as a listing of the experimentally derived values of D_{11} against laminated plate theory.

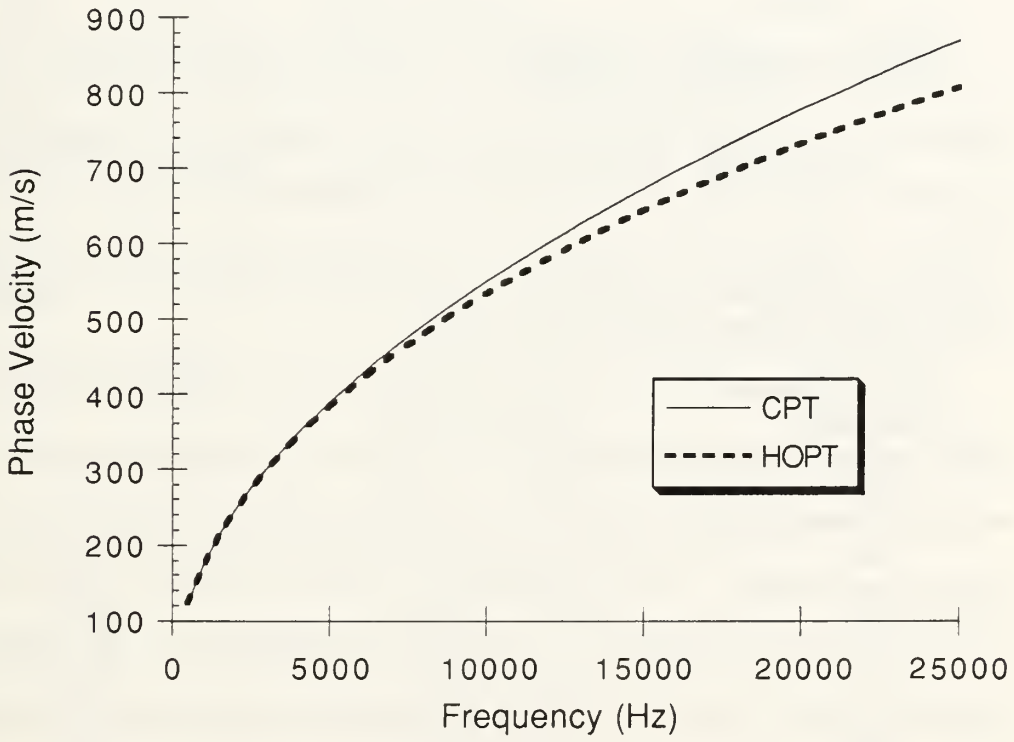

Figure 4.3 CPT vs. HOPT $[0,45,90,-45]_{2,s}$ laminate , 0° direction

The measurement at 10 kHz was not within experimental error of plate theory. However, the remaining measurements agree with theory within experimental error. To determine if the 10 kHz measurement represents a

systematic or random error, future studies should include statistical analyses using multiple measurements at the same frequency.

Table 4.3 $[0,45,90,-45]_{2,s}$ laminate, Experimental and Theoretical D_{11}

Frequency (kHz)	D_{11} (Nm) (experimental)	D_{11} (Nm) (plate theory)
6.0	83.6 (+/- 9.63)	84.3
7.0	86.0 (+/- 6.43)	84.3
8.0	82.7 (+/- 5.41)	84.3
9.0	90.7 (+/- 7.14)	84.3
10.0	66.8 (+/- 8.14)	84.3

CPT and HOPT agree within 5% if the experimental frequency is limited to 20.0 kHz when measuring in the 90° direction (Figure 4.4). Equation (4.2) was applied to recover D_{22} when limiting the experimental frequency to less than 20.0 kHz. Table 4.4 is presented as a listing of the experimentally derived values of D_{22} against laminate plate theory.

The experimental D_{22} was consistently lower than theory. As with the unidirectional laminate, this can be explained by the manufacturer's supplied material constants being higher than the as-manufactured experimental laminate's material properties. The measurement at 5 kHz was not within experimental error of the other measurements. Multiple measurements at the same frequency should be made in future studies to distinguish between systematic and random errors.

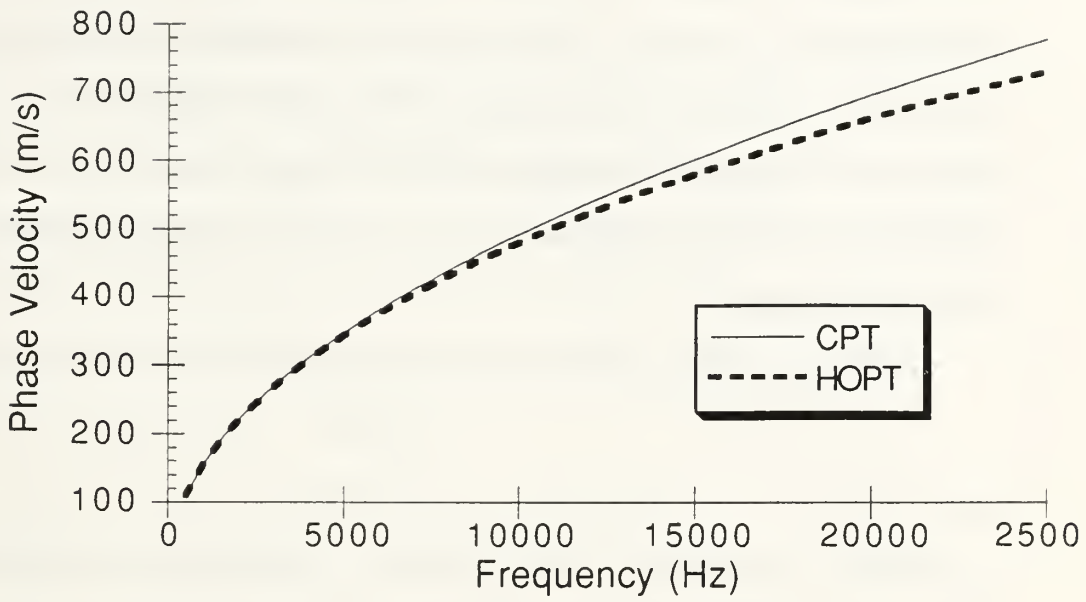

Figure 4.4 CPT vs. HOPT, $[0,45,90,-45]_{2,s}$ laminate , 90 direction

Table 4.4 $[0,45,90,-45]_{2,s}$ laminate, Experimental and Theoretical D_{22}

Frequency (kHz)	D_{22} (Nm) (experimental)	D_{22} (Nm) (plate theory)
4.0	42.9 (+/- 5.02)	58.3
5.0	51.88 (+/- 4.84)	58.3
6.0	44.56 (+/- 4.77)	58.3
7.0	41.0 (+/- 4.48)	58.3
8.0	43.2 (+/- 4.92)	58.3
9.0	40.5 (+/- 4.72)	58.3
10.0	45.0 (+/- 5.84)	58.3

In order to solve for the four unknown material properties (A_{44}, A_{55}, D_{16} and D_{66}), four measurements at four different frequencies in the 0° direction were made, thus resulting in four independent equations. Since equation 2.44 is nonlinear in terms of the material constants, a method to solve nonlinear equations was required. Wheatley [Ref. 16] describes how to reduce a nonlinear equation to a linear equation using a Newton's method approach which is summarized below.

We begin our discussion of non-linear systems by assuming two functions

$$f(x,y)=0,$$

$$g(x,y)=0.$$

Let x=r, y=s be a root. Both functions expanded as a Taylor's series about the point (x_i,y_i) in terms of (r-xi),(s-yi), where (xi,yi) is a point near the root, gives

$$f(r,s)=0= f(x_i,y)+ f_x(x_i,y_i)(r-x_i)+ f_y(x_i,yi)(s-yi)+ \ldots$$

$$g(r,s)=0= g(x_i,y_i)+ g_x(x_i,y_i)(r-x_i)+g_y(x_i,yi)(s-yi)+ \ldots \quad (4.7)$$

The subscript notation designates the partial derivatives. Truncating the series after the linear terms gives

$$\begin{bmatrix} 0 \\ 0 \end{bmatrix} = \begin{bmatrix} f(x_i,y_i) \\ g(x_i,y_i) \end{bmatrix} + \begin{bmatrix} f_x(x_i,y_i) & f_y(x_i,y_i) \\ g_x(x_i,y_i) & g_y(x_i,y_i) \end{bmatrix} \begin{bmatrix} r-x_i \\ s-y_i \end{bmatrix}. \quad (4.8)$$

The above equation can be rewritten to solve as the system of equations

$$\begin{bmatrix} f_x(x_i,y_i) & f_y(x_i,y_i) \\ g_x(x_i,y_i) & g_y(x_i,y_i) \end{bmatrix} \begin{bmatrix} \Delta x_i \\ \Delta y_i \end{bmatrix} = -\begin{bmatrix} f(x_i,y_i) \\ g(x_i,y_i) \end{bmatrix} \quad (4.9)$$

where Δx_i=r-xi and Δy_i =s-yi.

Equation (4.9) is solved by Gaussian elimination and an improved estimate of the root is made by setting

$$\begin{bmatrix} x_{i+1} \\ y_{i+1} \end{bmatrix} = \begin{bmatrix} x_i \\ y_i \end{bmatrix} + \begin{bmatrix} \Delta x_i \\ \Delta y_i \end{bmatrix} \quad (4.10)$$

The process is then iterated upon until f and g are close to zero.

A computer program was written in the BASIC language based upon the methods described by Wheatley.

However, this method never converged towards a solution. The non-convergence was due to the ill-conditioning of the partial derivative, square matrix of equation (5.9) as a result of the large magnitude differences between A_{44}, A_{55} (9.42 x 10^6 Pa m) and D_{16},D_{66} (19.9 Nm). The values of A_{44}/A_{55} were of a magnitude of a million times greater than the values of D_{16}/D_{66}.

C. $[0,90]_{4,S}$ LAMINATE

It was initially believed that for the cross-ply laminate at the experimental frequency required to recover D_{66}, the flexural mode would not be overpowered by the extensional mode. This was the limitation for the unidirectional laminate. The cross-ply laminate was analyzed next using the algorithm developed for the unidirectional plate since D_{16}=0. That is, using CPT in the lower frequency regimes where CPT and HOPT agree to recover D_{11} and D_{22}. HOPT is then used to recover the additional material constants.

CPT and HOPT agree within 5% if the experimental frequency is limited to 18 kHz when measuring in the 0° direction (Figure 4.5).

Equation (4.1) was applied to recover D_{11} when limiting the experimental frequency to less than 18 kHz. Table 4.5 is presented as a listing of the experimentally derived values of D_{11} against laminate plate theory.

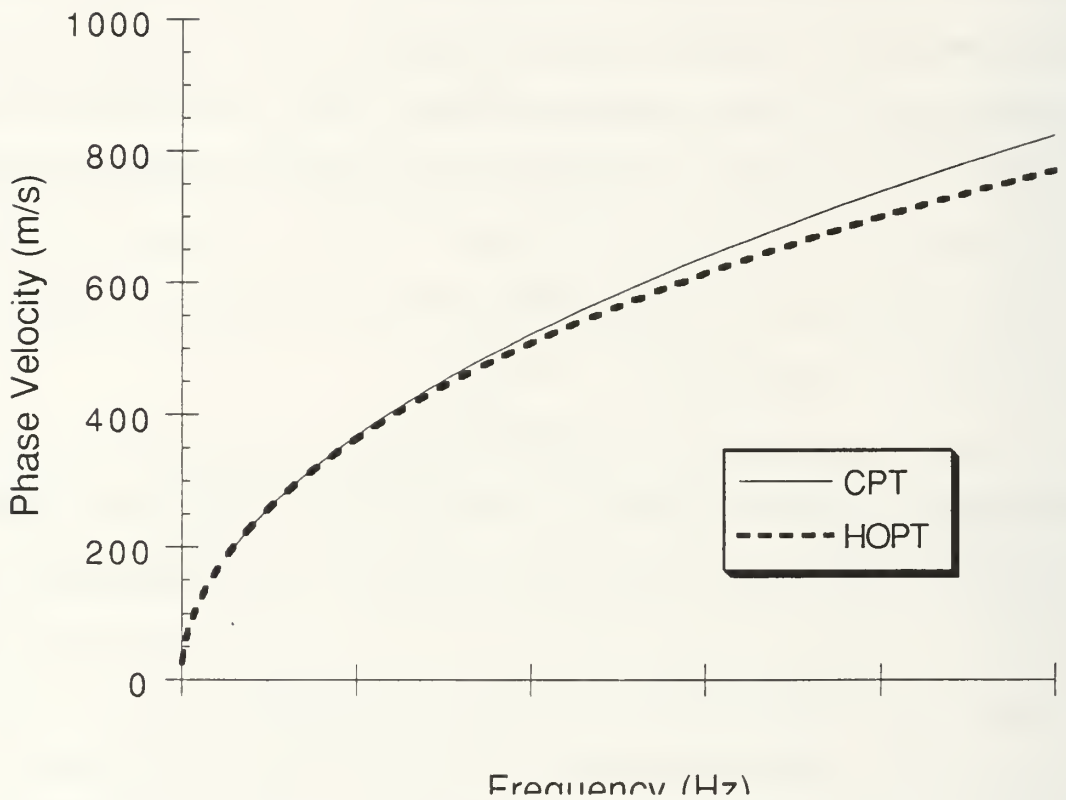

Figure 4.5 CPT vs. HOPT $[0,90]_{4,s}$ laminate , 0° direction

The measurements 8 and 14 kHz were not within experimental error of measurements made at the other frequencies. Statistical analyses using multiple measurements is necessary to distinguish between systematic and random errors.

Table 4.5 $[0,90]_{4,s}$ laminate, Experimental and Theoretical D_{11}

Frequency (kHz)	D_{11} (Nm) (experimental)	D_{11} (Nm) (plate theory)
8.0	60.3 (+/- 6.73)	113.0
10.0	92.3 (+/- 9.66)	113.0
12.0	88.6 (+/- 11.97)	113.0

14.0	69.9 (+/- 9.5)	113.0
16.0	83.3 (+/- 12.34)	113.0

CPT and HOPT agree within 5% if the experimental frequency is limited to 16.5 kHz when measuring in the 90 degree direction (Figure 4.6)

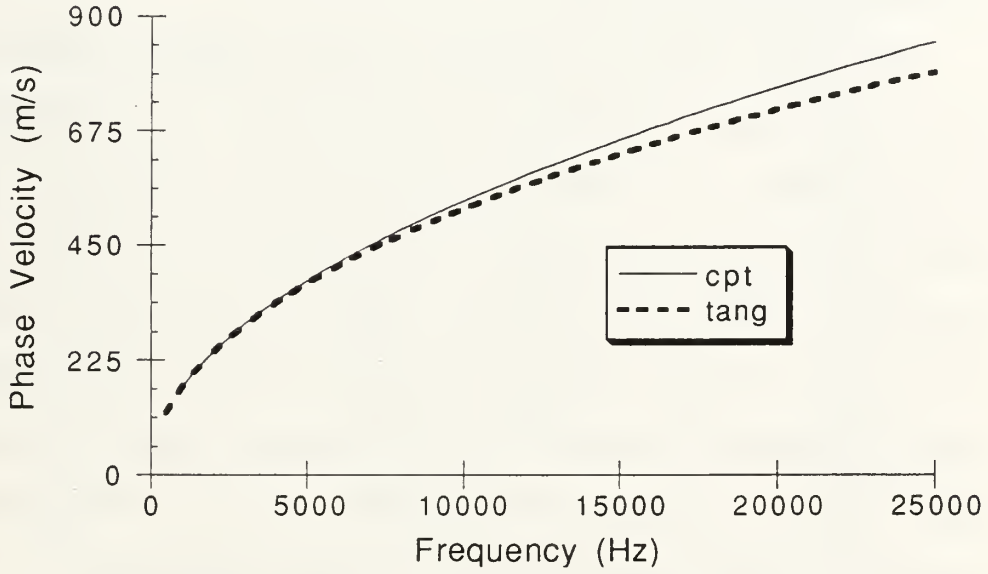

Figure 4.6 CPT vs. HOPT , $[0,90]_{4,s}$ laminate , 90° direction

Equation (4.2) was applied to recover D_{22} by limiting the experimental frequency to less than 16.5 kHz. Table 4.6 is presented as a listing of the experimentally derived values of D_{22} against laminate plate theory.

Table 4.6 $[0,90]_{4,s}$ laminate, Experimental and Theoretical D_{22}

Frequency (kHz)	D_{22} (Nm) (experimental)	D_{22} (Nm) (plate theory)
8.0	80.9 (+/- 9.45)	81.3

10.0	51.2 (+/- 5.98)	81.3
12.0	73.4 (+/- 9.60)	81.3
14.0	66.7 (+/- 9.05)	81.3
16.0	83.3 (+/- 12.34)	81.3

The measurement at 10 kHz was not within experimental error of the other measurements. Again, statistical analyses is necessary to differentiate between systematic and random errors.

From HOPT, equations (4.3) and (4.4) were applied to solve for A_{55} and A_{44}. The average experimental A_{55} was calculated to be 9.83 Mpa-m which compares nearly exactly with the theoretical value of 9.85 MPa-m. The average experimental A_{44} was calculated to be 7.80 MPa-m which is 20.8 % lower than the theoretical value of 9.85 MPa-m. Table 4.7 is presented as a listing of the experimentally derived values of A_{55} against theory while Table 4.8 is the experimentally derived values of A_{44} against theory. The small variation of the experimental A_{44} and A_{55} can be attributed to the less difficult measurement techniques required when measuring at the higher frequencies.

Equation (5.6) was utilized to attempt the recovery of D_{66}. However, similarly to the unidirectional laminate, when the experimental frequency was increased to excite the positive root of (5.6), the extensional mode dominated, making the measurement of the flexural mode impossible. Subsequently, D_{66} and ultimately D_{12} were not recoverable from this procedure.

Table 4.7 [0,90]$_{4,s}$ laminate, Experimental and Theoretical A_{55}

Frequency (kHz)	A_{55} (MPa-m) (Experimental)	A_{55} (MPa-m) (plate theory)
60.0	9.82 (+/- 1.07)	9.85
80.0	8.17 (+/-1.65)	9.85
100.0	9.98 (+/- 1.36)	9.85
120.0	9.89 (+/- 1.24)	9.85
130.0	10.11 (+/- 1.25)	9.85
140.0	10.33 (+/- 1.26)	9.85
150.0	9.94 (+/- 1.16)	9.85
160.0	10.47 (+/- 1.23)	9.85
170.0	9.94 (+/- 1.11)	9.85
180.0	9.37 (+/- 1.01)	9.85
190.0	9.93 (+/- 1.68)	9.85
200.0	10.04 (+/- 1.17)	9.85
220.0	9.69 (+/- 1.68)	9.85
240.0	9.83 (+/- 1.01)	9.85
260.0	9.84 (+/- 1.67)	9.85

Table 4.8 [0,90]$_{4,s}$ laminate, Experimental and Theoretical A_{44}

Frequency (kHz)	A_{44} (MPa-m) (Experimental)	A_{44} (MPa-m) (plate theory)
60.0	8.35(+/- 1.31)	9.85
80.0	7.26 (+/- 0.916)	9.85
100.0	7.42 (+/- 0.872)	9.85

110.0	7.39 (+/- 0.839)	9.85
120.0	7.66 (+/- 0.783)	9.85
130.0	7.74 (+/- 0.854)	9.85
140.0	7.97 (+/- 0.874)	9.85
150.0	7.86 (+/- 0.699)	9.85
160.0	8.01 (+/- 0.858)	9.85
170.0	8.02 (+/- 0.808)	9.85
180.0	8.00 (+/- 1.34)	9.85
190.0	7.86 (+/- 1.32)	9.85
200.0	7.90 (+/- 1.58)	9.85
210.0	7.69 (+/- 1.51)	9.85
220.0	7.8 (+/- 0.97)	9.85

D. DISCUSSION / SUMMARY OF ALGORITHMS TO RECOVER MATERIAL CONSTANTS

When first reviewing the procedures to recover the material constants, it was initially believed that the algorithm used for the unidirectional and cross-ply laminates would be sufficient. The employment of classical plate theory to recover D_{11} and D_{22} was attempted in all three laminates with limited success. Further work should include multiple measurements at the same frequency so statistical analyses can distinguish between systematic and random errors. The utilization of HOPT was successful to recover the transverse extensional terms A_{44} and A_{55} for the unidirectional and cross-ply laminates. The experimentally derived material properties were generally lower than values predicted by laminate plate theory. This is consistent with the experimentally measured phase velocities being generally lower than phase velocities predicted by HOPT.

Further analyses should also include comparisons between acoustically measured material properties to those derived from mechanical tests of specimens from the experimental laminates. The recovery of D_{66} dictated experimental frequencies where the extensional mode dominated making the measurement of the flexural mode impossible.

If D_{66} could have been recovered, the only material constant not accounted for would have been D_{12}. It would have possible to solve for D_{12} by the substitution of all known material constants and an off principal axis velocity measurements into equation (3.43).

The inability to recover D_{66} and D_{12} in the cross-ply and unidirectional laminates dictated the exploration of a new procedure to recover the material constants in the angle-ply laminate. It was determined that a new algorithm would be based upon equation (2.44). (2.44) was chosen because a significant simplification of the governing equation ensues when measuring wave propagation in the principle directions (0°or 90°). By successfully incorporating CPT at the lower frequency regimes, it was possible to recover D_{11} and D_{22}. The unknown material properties in (3.44) were reduced to 4 (A_{44}, A_{55}, D_{16} and D_{66}). A_{44} and A_{55} can not be calculated directly as before because D_{16} is not zero.

In order to solve for the four unknowns, four experimental conditions were input to produce four independent equations. These independent equations are nonlinear in terms of the material constants. A numerical method developed by Wheatley [Ref. 15] was then utilized to reduce a nonlinear equation to a linear equation using a Newton's method approach. Unfortunately, this method never converged towards a solution. The non-convergence was due to the ill-

conditioning of the partial derivative, square matrix of equation (4.9). It was later discovered that the large magnitude differences between A_{44}/ A_{55} and D_{16}/D_{66} is responsible for the ill-conditioning of the matrix.

Although this method base upon Wheatley did not converge, it is believed that a solution can be derived from a more robust numerical method. When factoring out equation (2.44) or (2.45), it can be proven that the equation is nearly quadratic in terms of the material properties. Reference 16 recommends several numerical methods to undertake to solve more advanced problems of this type. A methods which show promise is the Conjugate Direction method for non-linear systems.

Another method to attempt to solve for the material constants which shows promise but was not attempted due to time constraints is based upon equation (2.9) using classical plate theory. (2.9) can be solved using linear algebra since the equations are linear in terms of the material constants. By measuring phase velocities along principal directions in the lower frequency regimes, we have proven it is possible to recover D_{11} and D_{22}. The unknown material properties of equation (2.9) are reduced to three ,D_{12}, D_{16} =D_{26} (symmetric laminate only) and D_{66}. By measuring in off-principal directions at varying experimental frequencies, it will be possible to generate three linearly independent equations in terms of the unknown properties. This is the very approach that was attempted in the $[0, 45,90,-45]_{4,s}$ laminate that did not converge due to ill-conditioning. However, this situation is different in that all unknown parameters are roughly of the same magnitude which would prevent the ill-conditioning that occurred before. Also this numerical method represents a system of linear equations which is a significant simplification over a system of nonlinear systems.

V. SUMMARY

Composite materials promise to be a major structural material of the future. Composite materials present unique problems in that the complexities of the manufacturing process present increased opportunities for the introduction of defects. An ability to nondestructively determine the elastic properties of the composite component would be an invaluable tool for quality assurance. This thesis investigated a technique to yield the stiffness constants of composite laminates.

The initial aspect of this thesis was the verification of flexural wave propagation theory in composite laminates. Experimental phase velocities were measured in graphite/epoxy plates and were compared with dispersion curves calculated using higher order plate theory. Figures 3.3 through 3.9 summarize the results. The general trend of theory is observed but the phase velocities are typically lower than those predicted theoretically. This discrepancy could be explained if the actual elastic constants of these plates were smaller than those quoted by the manufacturer. An area for future analysis would be to compare acoustically measured material properties to those derived from mechanical tests of specimens from the experimental laminates.

The second aspect of this thesis was concerned with using the experimental phase velocities to determine the laminate material properties by inverting the governing equations. This turned out to be a very difficult problem for several reasons and different methods were tried. The first method incorporated Classical Plate Theory (CPT) to recover D_{11} and D_{22} and Higher Order Plate Theory (HOPT) to recover A_{44} and A_{55} for the unidirectional and cross-ply

laminates. However, at the higher frequencies necessary to recover D_{66} and D_{12} the extensional mode dominated making the measurement of the, flexural mode impossible.

The inability to recover D_{66} and D_{12} dictated the exploration of a new procedure on the $[0,45,90,-45]_{2,s}$ laminate. CPT was applied to recover D_{11} and D_{22}. By assuming wave propagation along a principal direction, the wave propagation equations were significantly simplified. The unknown material properties were reduced to four. Four experimental velocity measurements at different frequencies along the zero degree direction were input to produce four independent equations. The four equations can be solved for the four remaining unknown parameters. Because these equations are nonlinear in terms of the material constants, a nonlinear numerical method was utilized. Unfortunately, this method did not converge towards a solution due to the ill-conditioning of the matrix. Several other numerical methods were suggested in Chapter IV for further exploration.

A method proposed but not examined was to use non-principal direction velocity measurements in conjunction with classical plate theory (developed in Chapter 2) to recover D12, D16 and D_{66}. These measurements must be made at frequencies at which classical plate theory is valid. Previous measurements at the lower frequency regime have proven to be difficult but the numerical method to recover the unknown parameters would be greatly simplified because the equations are linear.

APPENDIX A- LAMINATE MATERIAL PROPERTIES

The dispersion curves were calculated using the following material properties of AS/4 3502:

E_{11}=144.8 GPa E_{22}=9.65 GPa G_{12}=5.97 GPa

ν_{12}=0.3 ν_{23}=0.34 .

All plates were assumed to have a density of 1550 kg/m^3.

The thickness of the $[0]_{16}$ plate was 0.002352 m.

The thickness of the $[0,90]_{4,s}$ plate was 0.0024688 m.

The thickness of the $[0,45,90,-45]_{2,s}$ plate was 0.0023368 m.

The calculated bending stiffnesses, Dij, for the $[0]_{16}$ laminate are :

D_{11}=113.0 Nm, D_{12}=3.65 Nm, D_{16}= D_{26}= 0.0 Nm,

D_{22}=81.4 Nm, D_{66}=7.49 Nm.

The calculated transverse extensional stiffnesses, Aij, for the $[0,90]_{4,s}$ laminate are A44=9.84Mpa. and A55=9.84 MPa.

The calculated bending stiffnesses, Dij, for the $[0,90]_{4,s}$ laminate are

D_{11}=113.0 Nm ,D_{12}=3.65 Nm, D_{16}= D_{26}= 0.0 Nm,

D_{22}=81.4 Nm , D_{66}=7.49 Nm.

The calculated transverse extensional stiffnesses, Aij, for the $[0,90]_{4,s}$ laminate are A44=9.84Mpa. and A55=9.84 MPa.

The calculated bending stiffnesses , Dij, for the $[0,45,90,-45]_{2,s}$ laminate are :

D_{11}=84.3 Nm D_{12}=1.67Nm D_{16}= D_{26} = 5.93 Nm

D_{22}=53.8 Nm D_{66}=19.9 Nm.

The calculated transverse extensional stiffnesses , Aij, for the $[0,45,90,-45]_{2,s}$ laminate are A44=9.42MPa and A55= 9.42 MPa.

The shear correction factors for composite laminates, $\kappa_1 \kappa_2$ were experimentally found to be 5/6 by Tang, Stiffler and Henneke [Ref. 12].

APPENDIX B - EXPERIMENTAL DATA

The transducers used for experimental measurements were:

A- Harisonic HC-483, resonant frequency 2.25 MHz, diameter 12.7 mm

B- Harisonic HC-483, resonant frequency 1.0 MHz, diameter 12.7 mm

C- Harisonic G0504 , resonant frequency 5.0 MHz, diameter 6.3 mm

D- Physical Acoustics Corp R15-3194, resonant frequency, diameter 12.7 mm

E- Accelerometer, diameter 12.7 mm.

N.A.- Not Available

Table 1. Experimental Phase Velocity Measurements

$[0,90]_{4,S}$ laminate , 0° propagation

Frequency (kHz)	distance, (m)	time difference (μs)	Phase Velocity (m/s)	Exciter/ Receiver Transducer
8.0	0.1	224	446.4	A/B
10.0	0.1	180	555.5	A/B
12.0	0.1	166	602.4	A/B
14.0	0.13	212	613.2	A/B
16.0	0.1	146	684.9	A/B
60.0	0.1	89.6	1116.1	A/B
80.0	0.1	84.8	1179.2	A/B
100.0	0.1	76.0	1314.0	A/B
120.0	0.1	72.8	1373.6	A/B

130.0	0.1	71.0	1408.4	C/C
140.0	0.1	69.4	1440.9	B/C
150.0	0.1	69.2	1445.0	B/C
160.0	0.1	67.2	1488.1	B/C
170.0	0.1	67.6	1479.3	C/C
180.0	0.1	68.4	1462.0	C/C
190.0	0.1	66.4	1506.0	C/C
200.0	0.05	32.8	1524.0	C/C
220.0	0.06	39.4	1522.8	C/C
240.0	0.1	64.6	1548.0	C/C
260.0	0.06	38.4	1562.5	C/C

Table 2. Experimental Phase Velocity Measurements

$[0,90]_{4,s}$ laminate , 90° propagation

Frequency (kHz)	distance, l (m)	time difference (μs)	Phase Velocity (m/s)	Exciter/ Receiver Transducer
8.0	0.05	104.0	480.7	A/B
10.0	0.07	146.0	479.5	A/B
12.0	0.1	174.0	574.7	A/B
14.0	0.1	165.0	606.0	A/B
16.0	0.05	73.0	684.9	A/B
60.0	0.1	93.6	1068.4	A/B

80.0	0.1	88.4	1131.2	A/B
100.0	0.1	83.2	1201.9	A/B
110.0	0.1	81.6	1225.5	A/B
120.0	0.11	87.2	1261.5	A/B
130.0	0.1	77.8	1285.3	A/B
140.0	0.1	76.0	1315.8	A/B
150.0	0.12	90.6	1324.5	A/B
160.0	0.1	74.0	1351.3	A/B
170.0	0.1	74.2	1347.7	C/C
180.0	0.06	44.1	1360.5	C/C
190.0	0.06	43.8	1369.8	C/C
200.0	0.05	36.2	1381.2	C/C
210.0	0.05	36.4	1373.6	C/C
220.0	0.08	57.4	1393.7	C/C

Table 3 Experimental Phase Velocity Measurements

$[0,45,90,-45]_{4,S}$ laminate , 0° propagation

Frequency (kHz)	distance,l (m)	time difference (μs)	Phase Velocity (m/s)	Exciter/ Receiver Transducer
20.0	0.1	157.0	700.0	N.A
30.0	0.1	151.0	827.0	N.A
40.0	0.1	103.0	970.0	N.A
60.0	0.1	91.2	1096.0	N.A

80.0	0.1	82.8	1207.8	N.A
100.0	0.1	78.0	1282.0	N.A
120.0	0.1	76.0	1315.0	N.A
140.0	0.1	74.2	1347.7	N.A
160.0	0.09	65.0	1384.6	N.A
180.0	0.1	70.0	1428.0	N.A
200.0	0.1	50.0	1500.0	N.A

Table 4 Experimental Phase Velocity Measurements

$[0,45,90,-45]_{4,s}$ laminate , 22.5° propagation

Frequency (kHz)	distance,l (m)	time difference (μs)	Phase Velocity (m/s)	Exciter/ Receiver Transducer
40.0	0.1	113.0	884.9	N.A
60.0	0.1	98.0	1020.4	N.A
80.0	0.1	85.6	1168.2	N.A
100.0	0.1	82.0	1219.5	N.A
120.0	0.1	76.6	1305.4	N.A
140.0	0.1	75.0	1333.3	N.A
160.0	0.1	72.2	1385.0	N.A
180.0	0.08	56.6	1413.4	N.A
200.0	0.08	54.8	1459.8	N.A

Table 5 Experimental Phase Velocity Measurements

$[0,45,90,-45]_{4,s}$ laminate , 45.0° propagation

Frequency (kHz)	distance,l (m)	time difference (μs)	Phase Velocity (m/s)	Exciter/ Receiver Transducer
30.0	0.1	128.0	781.25	N.A
40.0	0.1	119.0	840.3	N.A
60.0	0.1	100.8	992.1	N.A
80.0	0.1	91.2	1096.5	N.A
100.0	0.1	84.8	1179.2	N.A
120.0	0.1	81.2	1231.5	N.A
140.0	0.1	77.8	1285.3	N.A
160.0	0.1	74.8	1336.9	N.A
180.0	0.1	73.2	1366.1	N.A

Table 6 Experimental Phase Velocity Measurements

$[0,45,90,-45]_{4,s}$ laminate , 67.5° propagation

Frequency (kHz)	distance,l (m)	time difference (μs)	Phase Velocity (m/s)	Exciter/ Receiver Transducer
20.0	0.1	160.0	625.0	N.A
40.0	0.1	120.0	833.3	N.A

50.0	0.1	110.8	902.5	N.A
60.0	0.1	102.8	972.7	N.A
80.0	0.1	96.0	1041.0	N.A
100.0	0.1	86.6	1152.1	N.A
120.0	0.1	81.8	1222.5	N.A
140.0	0.1	80.4	1243.8	N.A
160.0	0.1	78.6	1272.3	N.A
180.0	0.1	75.0	1333.3	N.A

Table 7 Experimental Phase Velocity Measurements

$[0,45,90,-45]_{4,S}$ laminate , 90° propagation

Frequency (kHz)	distance,l (m)	time difference (μs)	Phase Velocity (m/s)	Exciter/ Receiver Transducer
20.0	0.1	156.0	641.0	N.A
30.0	0.1	135.0	740.7	N.A
40.0	0.1	121.0	826.4	N.A
60.0	0.1	102.8	972.8	N.A
80.0	0.1	92.4	1082.2	N.A
100.0	0.1	86.4	1157.4	N.A
120.0	0.1	82.8	1207.7	N.A
140.0	0.1	78.2	1278.7	N.A

160.0	0.1	77.6	1288.0	N.A
170.0	0.1	77.0	1298.7	N.A
180.0	0.1	75.2	1329.8	N.A

Table 8 Experimental Phase Velocity Measurements

$[0]_{16}$ laminate , 0° propagation

Frequency (kHz)	distance, l (m)	time difference (μs)	Phase Velocity (m/s)	Exciter/ Receiver Transducer
6.0	0.2	404.0	495.0	B/D
8.0	0.2	368.7	542.0	B/D
10.0	0.2	330.0	606.0	B/D

Table 9 Experimental Phase Velocity Measurements

$[0]_{16}$ laminate , 90° propagation

Freq (kHz)	distance,l (m)	time difference (μs)	Phase Velocity (m/s)	Exciter/ Receiver Transducer
6.0	0.1	392.0	255.1	B/E
8.0	0.1	320.0	312.5	B/E
10.0	0.1	292.0	342.5	B/E
100.0	0.1	113.6	880.3	B/E

APPENDIX C - EXPERIMENTAL ERRORS

Let R be a function of some independently measured quantities x1, x2, x3,...,xn. That is

$$R=R(x_1,x_2,x_3,...,x_n)\,. \qquad \text{(C-1)}$$

Let W_r be the uncertainty in the result, R, and W_1, W_2, ... W_n be the uncertainties in the independent variables. Then the uncertainty in the result is given in Ref. [15] as

$$W_R=\left[(\frac{\partial R}{\partial x_1}W_1)^2+(\frac{\partial R}{\partial x_2}W_2)^2+...+(\frac{\partial R}{\partial x_n}W_n)^2\right]^{1/2}. \qquad \text{(C-2)}$$

A. D11/ D22

For this application, the governing equation was

$$D_{11}=(\frac{V_p{}^4\rho h}{4\pi^2 f^2})\,. \qquad \text{(C-3)}$$

The phase velocity, V_p, was divided into the experimental measurements of distance and time difference , Δt.

$$Vp=\frac{\Delta dist}{\Delta t}. \qquad \text{(C-4)}$$

The density, ρ , was likewise divided into the experimental measurements of mass and volume (length, width and height).

$$\rho=\frac{kg}{volume}=\frac{kg}{l_1 l_2 h}. \qquad \text{(C-5)}$$

Substituting experimental measurements (C-4) and (C-5) into (C-3) gives

$$D_{11}=\frac{V_p{}^4\rho h}{4\pi^2 f^2}=\frac{(dist)^4(kg)h}{(\Delta t)^4(4\pi^2 f^2)l_1 l_2 h}. \qquad \text{(C-6)}$$

Canceling the height, h, results in

$$D_{11}=\frac{(dist)^4(kg)}{(\Delta t)^4(4\pi^2 f^2)l_1 l_2}. \qquad \text{(C-7)}$$

The following experimental uncertainties were assumed when measuring at the lower frequency regimes:

(A) dist=dist +/- 0.002m

(B) kg= kg +/- 0.0001 kg

(C) $\Delta t = \Delta t +/- 5\mu s$

(D) $l_1 = l_1 +/- 0.001$m

(E) $l_2 = l_2 +/- 0.001$m

(F) experimental error from input frequency was small in comparison to other experimental parameters and thus was neglected.

After partial differentiation in terms of the independent variables, the uncertainty in the experimental result of D_{11} was

$$\Delta D11 = [(\frac{4(dist)^3 kg}{\Delta t^4 4\pi^2 f^2 l_1 l_2}\Delta dist)^2 + (\frac{(dist)^4}{\Delta t^4 4\pi^2 f^2 l_1 l_2}\Delta kg)^2 + (\frac{4(dist)^4 kg}{\Delta t^5 4\pi^2 f^2 l_1 l_2}\Delta t)^2$$
$$+(\frac{(dist)^4 kg}{\Delta t^4 4\pi^2 f^2 l_1^2 l_2}\Delta l_1)^2 + (\frac{(dist)^4 kg}{\Delta t^4 4\pi^2 f^2 l_1 l_2^2}\Delta l_2)^2]^{1/2}. \quad (C\text{-}8)$$

Substituting experimental data and uncertainties into (C-8) gives experimental errors for D11 quoted in Chapter IV.

The same procedures and uncertainties were used for the calculation of experimental error in D_{22}.

B. A44/ A55

The governing equation for the calculation of A55 was

$$A_{55} = \frac{\rho^{\cdot}\omega^2(D_{11}k^2 - I\omega^2)}{D_{11}k^4 - \rho^{\cdot}\omega^2 - I\omega^2 k^2}. \quad (C\text{-}9)$$

$\rho^{\cdot}$ was divided into the experimental measurements of mass (kg.) and the length and width of the plate resulting in

$$\rho^* = \rho h = \frac{kg}{l_1 l_2}. \quad (C\text{-}10)$$

The inertia term, I, was similarly divided into the experimental measurements of mass, height, length and width, resulting in

$$I = \frac{h^2 kg}{12 l_1 l_2}. \qquad \text{(C-11)}$$

(C-10), (C-11) and (C-4) were substituted into (C-9), resulting in the following experimental expression of A55:

$$A_{55} = \frac{\left(\frac{16 D_{11} k g \pi^4 f^4 \Delta t^4}{l_1 l_2 (dist)^4} - \frac{16 k g^2 h^2 \pi^4 f^4}{12 l_1^{\,2} l_2^{\,2}}\right)}{\frac{16 D_{11} \pi^4 f^4 \Delta t^4}{dist^4} - \frac{4 k g \pi^2 f^2}{l_1 l_2} - \frac{16 D_{11} k g h^2 \pi^4 f^4 \Delta t^4}{12 l_1 l_2 dist^2}}. \qquad \text{(C-12)}$$

In accordance with (C-2), (C-12) was differentiated with respect to the experimental parameters. All experimental uncertainties from D11 were maintained except that the time difference uncertainty, Δt, was reduced to +/- 1 μs because the output signal was much clearer when measuring at the higher frequencies and the laminate height measurement uncertainty was small and thus neglected. Experimental data and uncertainties were input to determine experimental uncertainties quoted in Chapter IV.

The same uncertainties and procedures were used to calculate the experimental uncertainties of A44.

LIST OF REFERENCES

1. American Society for Testing and Materials , *Composite Materials: Testing and Design*, pp.-2, 1971

2. Jones, R.M., *Mechanics of Composite Materials*, pp. 1-29, Hemisphere Publishing Corporation, 1975

3. Tsai, S.W. , *Composites Design 1986*, pp.-6, Think Composites, 1986

4. Middleton, D.H., *Composite Materials in Aircraft Structures*, pp.1-15 and pp. 190-205, Longman Scientific and Technical, 1990

5. Dayal, V., and Kinra, V.K., "Leaky Lamb Waves in an Anisotropic Plate. I: An Exact Solution and Experiments ," Journal of the Acoustical Society of America, v. 85, n.6, pp. 268-2276, June 1989

6. Every, A.G. and Sachse, W. " Determination of the Elastic Constants of Anisotropic Solids from Acoustic-Wave Group-Velocity Measurements," Physical Review, v.42, n.13, pp. 8196-8205, 1 November 1990

7. Wu,T.T., and Ho,Z.H. , "Anisotropic Wave Propagation and its Applications to NDE of Composite Materials," Experimental Mechanics, v.30, n,4 pp. 313-318

8. Wu, T.T., and Chiu, S.T., "On the Propagation of Horizontally Polarized Shear Waves in a Thin Composite Laminate Plate," Ultrasonics, v. 30, n.1, 1992, pp. 60-64

9. Castagnede, B., Kim,K.Y., and Sachse, W., "Determination of the Elastic Constants of Anisotropic Materials using Laser-Generated Ultrasonic Signals," Journal of Applied Physics, v.70, n.1, 1 July 1991, pp. 150 -157

10. Every, A.G. and Sachse, W., "Sensitivity of Inversion Algorithms for Recovering Elastic Constants of Anisotropic Solids from Longitudinal Wavespeed Data," Ultrasonics, v. 30, n.1,1992 ,pp. 43-47

11. Gorman, M.R. "Plate Wave Acoustic Emission," Journal of the Acoustic Society of America, v.90, n.1 July 1991, pp. 358-364

12. Tang,B., Henneke II, E.G., and Stiffler, R.C., "Low Frequency Flexural Wave Propagation in Laminated Composite Plates," journal of Composite Materials, v.23, n. 2, pp. 195-206

13. Graff, Karl F., *Wave Motion in Elastic Solids,* Ohio State University Press, 1975

14. Mindlin, R.D., "Influence of Rotary Inertia and Shear Flexural Motions of Isotropic, Elastic Plates," Journal of Applied Mechanics, v. 18, pp. 31-38, March 1951

15. Holman, J.P., *Experimental Methods for Engineers*, Fifth Edition, pp. 37-49, McGraw -Hill Publishing Company, 1989

16. Wheatley, C.F. and Gerald ,P.O., *Applied Numerical Methods,* Fourth Edition, pp. 141-147, Addison-Wesley Publishing Company, 1989

17. Greenspan, D. and Rozsa,P., *Numerical Methods,* pp. 481-502, North Holland Publishing Company, 1988

INITIAL DISTRIBUTION LIST

1. Defense Technical Information Center Cameron Station Alexandria, VA 22304-6145	2
2. Library, Code 0142 Naval Postgraduate School Monterey, CA 93943-5000	2
3. Prof. Michael R. Gorman 916 E. Phillips Lane Littleton, CO 80122	6
4. Prof. Edward M. Wu Code AA/WU Naval Postgraduate School Monterey, CA 93943-5000	1
5. Dr. Steven M. Ziola 4363 So. Quebec St. #2313 Denver, CO 80237	1
6. .Dr. William H. Prosser NASA Langley Research Center Mail Stop 231 Hampton, VA 23665	1
7. Dr. Ajit K. Mal MANE 405 Hilgard Ave. UCLA Los Angeles, CA 90024-1527	1

8. LT. Brian B. Elliott 1

539 Sangree Rd.

Pittsburgh, PA 15237